MAX IV Beamline Review Report

NanoMAX

April 2021

NanoMAX Beamline Review Report

The NanoMAX team* and MAX IV User Office†

2021-04-20

Preface

This report is compiled to facilitate the 2021 review of the NanoMAX beamline. It describes the design, realization, performance, operation, and strategy for the future. Specifically, it aims to provide the background needed for the committee to assess the beamline across the following four areas.

- The Technical realization of the beamline and endstation, in terms of performance and competitiveness.
- The engagement with and fostering of the user community, as well as the impact and scientific productivity.
- Beamline operation, quality and extent of support and surrounding infrastructure.
- The outlook for the future, including upgrade plans, development, and scientific strategy.

Contents

*Alexander Björling, Ulf Johansson, Maik Kahnt, Sebastian Kalbfleisch, Simone Sala, Karina Thånell
†Franz Hennies

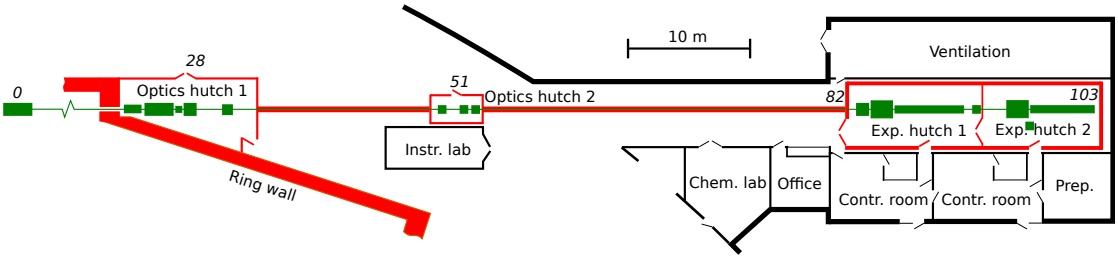

Figure 1: NanoMAX floor plan. The beamline is shown in green on the main and satellite buildings. Red indicates radiation-controlled hutches and the shielded beam-transportation tube. Approximate distances from the undulator are shown in italics.

1 Technical Description

1.1 Beamline introduction

NanoMAX is currently the only hard x-ray nanoprobe beamline at MAX IV, and is therefore designed to accommodate a wide range of imaging and scattering methods, which are either based on the use of a focused coherent beam to achieve ultimate resolution, such as eg., ptychography and coherent diffraction imaging (CDI), or where the nano-focused beam provides prime spatial resolution, such as scanning diffraction and X-ray fluorescence (XRF) mapping experiments [1]. NanoMAX serves diverse interests in science, where the common denominator is the use of nano-focused X-rays for imaging, scattering and/or spectroscopic investigations. In its fully developed form, the beamline will therefore accommodate two endstations to allow for this broad range of user experiments and their respective demands on the sample environment. The first *diffraction endstation*, brought into operation in 2017, has Kirkpatrick-Baez (KB) mirror focusing of $40 - 200$ nm, scaling inversely with the photon energy (5-28 keV), and is designed around the need for flexible sample environments and detector configurations - currently in air, and at room temperature. The modular and open nature of this endstation also provides opportunities for testing new methods and experimental configurations. Currently, the three main categories of methods regularly used are: CDI in forward and Bragg geometries, nano-diffraction in both geometries, and 2D XRF imaging. Examples of experiments performed so far are diffraction and strain mapping of nano-wires, single nano-particle coherent Bragg imaging, extreme pressure nano-diffraction, ptychographic tomography, 2D XRF imaging of plant, animal and human cells, nano-diffraction of polycrystalline materials, and X-ray technology development. The second, in vacuum *tomography endstation*, based on Fresnel zone plate (FZP) optics, is currently under development. It will be somewhat less modular and optimized to provide highest possible spatial resolution ($10 - 50$ nm) for 2D and tomographic experiments with XRF, XANES contrast, and CDI as primary imaging methods and feature liquid nitrogen cooling to mitigate radiation damage in sensitive samples. The beamline has several detectors that can be shared between the two endstations and a configurable control system to allow integration of user equipment.

NanoMAX is located in sector three of MAX IV's twenty-fold symmetric, 3 GeV, 528 m circumference, storage ring. The beamline area is shown in Figure 1 and the main storage ring and beamline parameters are listed in Table 1. The beamline is approximately 100 meters long and extends out of the main experimental hall into a satellite building.

Table 1: Main parameters of the MAX IV 3 GeV storage ring and NanoMAX beamline.

Storage ring energy	3 GeV
Nominal design current	500 mA
Current (Operation Apr 2021)	250 mA
Electron beam emittance	326 pm rad (x), 8 pm rad (y)
Electron energy spread	7.7×10^{-4}
Electron source size	54 µm(σ_x), 4 µm(σ_y)
Electron source divergence	6 µrad (σ_x), 2 µrad (σ_y)
Insertion device	In-vacuum undulator
Photon energy range	$5 - 28$ keV
Beamline optics	Vertical and horizontal focusing with mirrors onto secondary source
Monochromator	Cryo-cooled Si(111), double crystal, horizontally diffracting geometry
Endstation 1	In-vacuum tomography station with Fresnel zone-plate optics for highest resolution (under development)
Endstation 2	Versatile coherent diffraction station with Kirkpatrick-Baez optics (operational)
Detectors	Eiger 2X 4M, Merlin Si Quad 512K, Pilatus 2 1M, XRF SiriusSD 1-element SDD, Crycam X-ray camera with Andor Zyla 4.2+

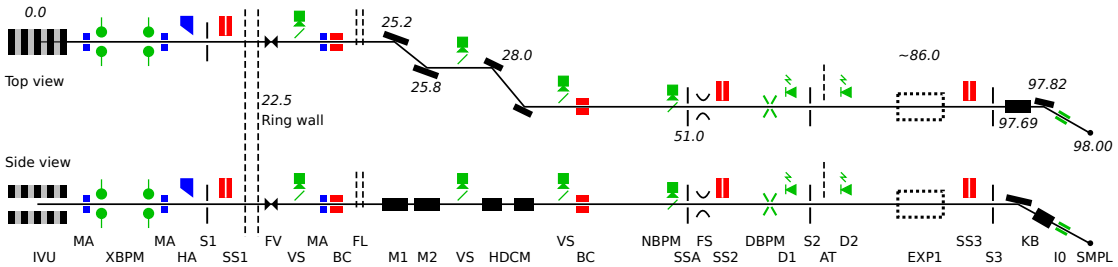

Figure 2: Top and side views of the beamline optics together with most components for diagnostics and beam conditioning along the beamline. Approximate distances in meters from the undulator are shown adjacent to main components. IVU: in-vacuum undulator, MA: heat absorbing masks, XBPM: X-ray blade beam position monitor (BPM), HA: actuated heat absorber, S1: L-shaped movable masks, SS1-3: radiation safety shutter, FV: fast closing valve, VS: fluorescence view screens, BC: bremsstrahlung collimators, FL: diamond heat filters, M1: vertically focusing mirror, M2: horizontally focusing mirror, HDCM: horizontal double crystal monochromator, NPBM: high-resolution BPM, SSA: secondary source aperture, FS: fast shutter, DBPM: diamond-BPM, D1-2: pin-diodes, S2: slits, AT: multiple attenuators, EXP1: place for tomography endstation, S3: KB-slits, KB: nano-focusing mirrors, I0: miniature ion-chamber, SMPL: sample position.

1.2 Source and optics

1.2.1 Undulator and front-end

The undulator is designed to be a brilliant source in the $5 - 28$ keV range. It has an in-vacuum, room temperature, permanent magnet design with a maximum K-value of 2.10. The physical length of the undulator is 2.8 meter long, although the straight section is 4 meter long. The choice for a shorter undulator was made in order to not challenge the initial operation of the ring and for easier heat load management. The undulator can be tapered to broaden undulator peaks, which can be useful in energy scanning experiments.

The heat load from the undulator, maximum 6.5 kW at 500 mA, is mainly handled in the front-end through fixed and adjustable masks and the beam acceptance angle is simultaneously reduced. Further heat load reduction, to a maximum of 100 W, takes place in the first optics hutch by reducing the angular acceptance angle of the white beam to 50 µrad (H) $\times$ 40 µrad (V), before the beam enters the mirror chamber.

1.2.2 Primary optics

The beamline optics layout is schematically depicted in Figure 2, together with most heat load (blue), radiation safety (red) and diagnostics components (green). We have realized an optical layout with few optical components where highest possible stability and simple operation have been prioritized. All optical components are deflecting the beam in the horizontal direction which favours beam stability since sensitivity to angular motions is lower in this direction due to the elliptical shape of the source. Two water-cooled white beam mirrors, M1 and M2 (see Table 2), are focusing the undulator source, in vertical respective horizontal direction, into a secondary source. A double crystal Si(111), fixed exit, monochromator is placed directly after the two main focusing mirrors. Directly after the monochromator, in the main optics hutch, space is reserved for a possible future upgrade with a multilayer monochromator. A high-precision slit system at the secondary source plane (secondary source aperture, SSA) defines the source for

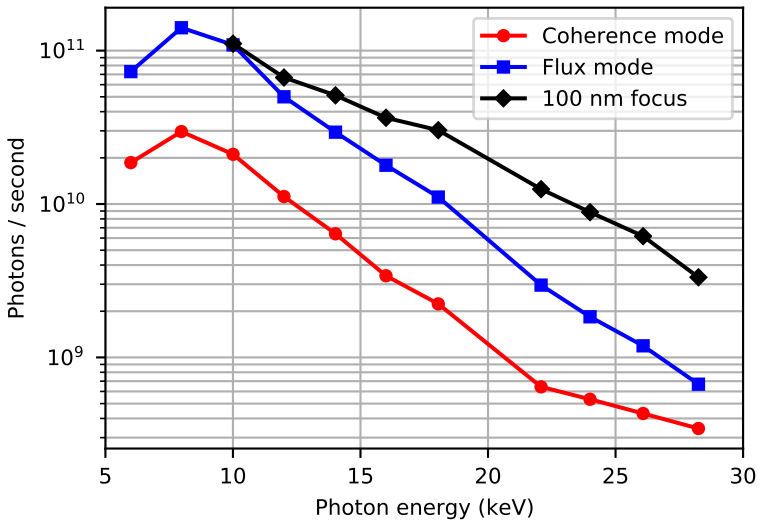

Figure 3: Photon flux measured at the sample position with a PIN diode for different SSA settings and energies at 250 mA ring current. Red curve: flux for highest degree of coherence. Blue curve: flux at lower degree of coherence but with approximately the same focus spot size as for high coherence. Black curve: flux for SSA opening resulting in approximately 100 nm spot size for energies above 10 keV.

the nano-focusing optics employed at the experimental stations. The SSA opening is used to control the transverse coherence length illuminating the FZP:s or KB-optics. By matching the coherence length to the acceptance aperture of the optics, diffraction limited focusing can be reached, or by opening the SSA, higher flux and larger spot size can be chosen, all to best suit the conducted experiment.

1.2.3 Kirkpatrick-Baez optics

The diffraction endstation uses ultimate quality reflective X-ray optics (see Table 2, JTEC, Japan) in a Kirkpatrick-Baez arrangement to focus the X-ray beam to $40-200$ nm. KB mirrors give a large energy range, long focal distance permitting various sample environments, achromatic focal distance allowing easy energy change and spatial resolution reaching the diffraction limit. The KB-mirrors have been optimized to reach the same numerical aperture and thereby resolution in vertical and horizontal direction. Incidence angles are optimized to give good reflectivity for the large energy range. The free distance between the KB-chamber exit window and the sample position is ~ 115 mm.

Figure 3 shows photon flux curves measured with a PIN diode at the sample position, for different SSA settings and energies at the nominal ring current 250 mA. The 3 GeV ring operates at 250 mA today, and will do so for the foreseeable future, but it is designed for 500 mA.

Spatial resolution can be measured in several direct ways, for example with knife-edge scans, imaging of test patterns revealing contrast, or indirectly by ptychography and probe reconstruction. In Figure 4 a Siemens star test chart (XRESO-50, NTT-AT, Japan) was measured with ptychography (A, B) and in total yield fluorescence (C, D) at two photon energies. The ptychographic measurement was done in *coherence mode* at 10 keV. The finest 50 nm spokes are clearly visible as expected because in ptychograpy the resolution is not limited to the focused beam

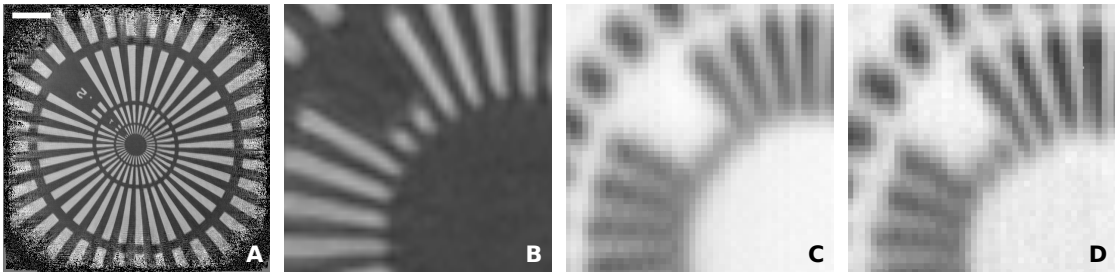

Figure 4: Ptychographic and direct spatial resolution measurement of a Siemens star pattern in Tantalum. (A) Ptychography reconstructed image of the Siemens star measured at 10 keV. (B) Close-up of the 50 nm in figure A. (C) Total yield fluorescence emission of the 50 nm central features measured at 10 keV excitation energy. (B) As in C but measured at 22 keV. Scalebar is 2 µm.

size but by scattering angle, shot noise, scanning accuracy, instrument stability, and ultimately wavelength. In Figure 4 C and D where the X-ray focus size determines the resolution, the finest details are clearer at 22 keV (D) compared to at 10 keV (C). This is in agreement with estimated focus sizes of 41 nm at 22 keV and 90 nm at 10 keV.

1.3 Comparison to other beamlines

Most synchrotron facilities that produce hard X-rays feature one or more nanoprobe beamlines. Some offer a wide variety of methods and configurations while others are highly specialized, such as those at large facilities which often host more than one nanoprobe. NanoMAX was funded under the assumption that it would remain the only nanoprobe beamline at MAX IV for a number of years, which is why two endstations were included in the original design. The idea was to cater to both condensed matter physicists in need of nanobeam diffraction and strain imaging, to biologists interested in nanotomography and high-resolution spectral characterization under cryogenic conditions, and to every nanobeam experiment in between. The broad scope sets NanoMAX apart from many of its competitors, some of which are summarized in Table 3.

Compared to other beamlines, NanoMAX has had the immediate advantage of being located at the world's first fourth-generation storage ring. This has meant a head start as, until the ESRF-EBS recently opened, no other nanoprobe beamline had been able to offer a coherent and nano-focused beam with $\sim 10^{10}$ ph/s. This is now changing with upgrades of several 3$^{\text{rd}}$ generation synchrotrons, including ESRF-EBS, PETRA IV, APS-U, and SLS-2, and the emergence of SIRIUS.

The diffraction endstation (section 1.4) is perhaps most naturally compared with other nanoprobe instruments which emphasize crystallography and strain imaging. It partly resembles, and is indeed inspired by, the ESRF beamline ID01, which also admits user-provided reactors and cells for in-operando experiments. That instrument also features a two-circle goniometer, but the Bragg condition is found using a classic detector arm rather than a robot. ID01 uses a range of focusing optics, with both refractive lenses, diffractive zone plates, and reflective and bendable KB mirrors. Here, the fixed JTEC mirrors at NanoMAX offer an advantage, as they provide a relatively stable diffraction-limited focus with a minimal number of degrees of freedom (see section 1.4). After the ESRF-EBS upgrade, ID01 is expected to produce a coherent flux comparable to or slightly exceeding that found at NanoMAX.

Another relevant nanoprobe comparison is the Soleil beamline Nanoscopium, which as a

Table 2: Mirror parameters

Primary mirror M1	Vertical focusing
Mirror shape	Fixed, circular cylinder
Radius, sagittal	68.9 mm
Incidence angle	2.7 mrad
Slope error	0.5 µrad RMS
Optical length	400 mm
Coating	Pt, 40 nm

Primary mirror M2	Horizontal focusing
Mirror shape	Bendable, circular cylinder
Radius, meridional	9.44 km
Incidence angle	2.7 mrad
Slope error	0.3 µrad RMS
Optical length	400 mm
Coating	Si, Rh, Pt, 40 nm

KB mirror KB-M1	Vertical focusing
Mirror shape	Fixed, elliptical cylinder
Source to mirror centre	46.69 m
Mirror centre to focal point	0.31 m
Incidence angle at mirror centre	2.7 mrad
Active optical surface (L x W)	140×8 mm
Figure error (tangential)	<1.0 nm PV
Micro roughness	<0.15 nm RMS
Reflective coating	Pt, $40 - 50$ nm
Geometrical demagnification	150.6

KB mirror KB-M2	Horizontal focusing
Mirror shape	Fixed, elliptical cylinder
Source to mirror centre	46.82 m
Mirror centre to focal point	0.18 m
Incidence angle at mirror centre	2.5 mrad
Active optical surface (L x W)	90×8 mm
Figure error (tangential)	<1.0 nm PV
Micro roughness	<0.15 nm RMS
Reflective coating	Pt, $40 - 50$ nm
Geometrical demagnification	260.1

nanoprobe at a smaller facility has also chosen to offer two endstations in order to broaden the overall portfolio. As for NanoMAX, the first is fitted with KB-optics for multi-modal imaging with spatial resolution down to 70 nm and generous sample space. The other uses FZPs for down to 35 nm resolution. Experimental methods used at both stations are ptychography, near edge spectroscopy and X-ray fluorescence mapping. The experimental program is to a large extent targeted towards imaging within the applied fields of environmental, biological, and geological sciences. As such, the beamline appears to offer a broad variety of instruments, like NanoMAX, but to have chosen a narrower scientific program.

The tomography endstation (section 4.1 below) at NanoMAX has its counterparts in specialized X-ray microscopes which focus heavily on imaging. The emphasis on tomography and a high degree of real-space control via advanced interferometry is reminiscent of the P06 endstations at PETRA III. That beamline features two endstations, both of which provide a variety of focusing optics. The so-called microprobe endstation delivers beams on the order of one or a few hundred nanometers, and provides spectral and fluorescence mapping (using the acclaimed Maia detector) as well as coherent imaging, with unusually long detector distances possible. The P06 nanofocus endstation, much like the NanoMAX tomography instrument, is built to provide optimal ptychographic tomography by maximizing sample stability at the expense of flexibility, and by reducing background scattering to a minumum. The latter is achieved using an evacuated detector tank, similar to that now in operation at NanoMAX. Although the endstations do not correspond one to one, the successful P06 strategy of providing one flexible and one more optimized tomography endstation is in part paralleled at NanoMAX. Lastly, the in-vacuum sample placement and nitrogen cooling for protecting the sample, are inspired by such instruments as ID16A (ESRF) and the OMNY instrument at cSAXS (SLS), while setting a level of ambition adapted to the resources available at MAX IV.

In summary, in the landscape of nanoprobe and coherent imaging beamlines, NanoMAX will, with both endstations fully operational, overlap with both specialized diffraction beamlines and imaging instruments from worldwide labs. This is a broad commitment brought about by the dual-endstation design and the burden of being the only hard X-ray nanoprobe at MAX IV. The challenge of staying competitive as more and more synchrotrons upgrade to fourth generation technology will require dedication, priorities, and maximally leveraging the user community.

1.4 Diffraction endstation

The diffraction endstation is in user operation since 2017 [2]. It is designed to provide an X-ray focus size in the $40 - 200$ nm range, using the full energy range, and to be highly configurable for various user experiments with emphasis on diffraction and scattering using custom sample setups. The location in the second experimental hutch, at ~ 47 meter distance from the SSA, allows for a relatively long working distance between the KB-focusing optics and sample position. The location also has the practical advantage that experimental preparations, which are likely to be lengthier and more frequent at the diffraction station than for the tomography station, can take place while an experiment is running in the first hutch.

The endstation is designed around the KB-optics and a two circle sample goniometer (see Figure 6). The mirror chamber and the goniometer are supported on a common 7 t granite block which is grouted to the floor. Experiments in the Bragg geometry require a photon counting pixel detector placed at an off-axis angle. Instead of using a detector arm which rotates around the sample position, common on diffraction endstations, we use an industrial robot (Cybertech KR20 R1810, Kuka, Germany) for positioning the detector (Merlin 250k, Quantum Detectors, UK) at the Bragg peak of interest. The mechanical precision was characterized by the robotics department at Lund University and its kinematical model was refined. The accuracy of the

Table 3: A selection of comparable nanoprobe hard X-ray beamlines. Photon flux numbers have been collected from published papers, beamline homepages and other sources, and might not offer a full comparison.

Beamline	Total flux	coherent flux	spot size	Optics
MAX IV - NanoMAX	$\sim 10^{11}$ ph/s	2×10^{10} ph/s	90 nm	KB
APS - 13-ID-B	3.5×10^{9} ph/s		70 nm	FZP
APS - 26-ID-C	1×10^{9} ph/s	$\sim 10^{7}$ ph/s	30 nm	FZP
PETRA III - P06 nano	1×10^{10} ph/s	$\sim 10^{7}$ ph/s	≈ 80 nm	NFL, MLL, CRL, FZP
Diamond - I14	5.4×10^{9} ph/s		50 nm	KB
ESRF-EBS - ID01		1×10^{10} ph/s	100 nm	FZP
ESRF - ID16A	4×10^{12} ph/s	6×10^{9} ph/s	13 nm	KB
NSLS-II - HXN		5×10^{8} ph/s	$10 - 50$ nm	MLL, FZP
SLS - cSAXS		7×10^{8} ph/s		FZP
Soleil - Nanoscopium	$\sim 10^{10}$ ph/s		$50 - 1000$ nm	KB

robot was then measured to be 180 µm, and the repeatability to be 20 µm. The detector robot is programmed to be conveniently positioned by applying polar coordinates with the sample position as origin. A vacuum flight tube downstream of the sample houses a photon counting pixel detector (Eiger2X 4M, Dectris, Switzerland). The forward sample-to-detector distance can be varied from 1.0 to 4.5 meters by adding or removing sections in the flight tube. An optical breadboard beside the flight tube can be moved in to the forward direction to support temporary detector setups, while parking the flight tube to the side. For example the beamline's scintillator X-ray camera (CRYCAM, Crytur, Czech Republic), the pixel detector (Pilatus 2 1M, Dectris, Switzerland) used for wide-angle X-ray scattering (WAXS) measurements or a user supplied detector can be mounted here. An XRF detector (SiriusSD 1-element, RaySpec, UK) and a high performance pulse processor (Xspress3, Quantum Detectors, UK) is available. The XRF detector is normally used in air, in the horizontal plane, at 60-90° angle to the incident X-ray beam.

Two optical microscopes with a resolution of ≈ 3 µm are used to navigate the sample to the measurement position. One microscope views the sample in the beam direction via a 45° mirror with a 0.6 mm through hole. A cross-hair placed in the microscope image indicates the position of the X-ray focus, which makes sample positioning simple. The second microscope views the sample from above which is useful for alignment purposes, e.g. finding centre of rotation, or in diffraction and tomography experiments. The free distance between the mirror chamber exit window and the sample position is ~ 115 mm. Within that section, a clean-up aperture and a small ion chamber for monitoring the beam intensity, and the mirror for the optical microscope is located. The practical free distance for custom sample environments is approximately 50 mm, but by moving the above mentioned components out, larger environments can be fitted.

The two-circle goniometer of the diffraction endstation is a $\vartheta - \varphi$ assembly. It provides a 360° rotation of the azimuthal angle φ and a rotation of ϑ in the range from $-2°$ to 90°. The sphere of confusion over the full travel range is less than 6 µm. Over the typical scan range of a rocking curve the run-out is below 100 nm. To benefit from the low run-out, the center of rotation has to coincide with the X-ray focus. For this a set of motorised adjustment legs underneath and

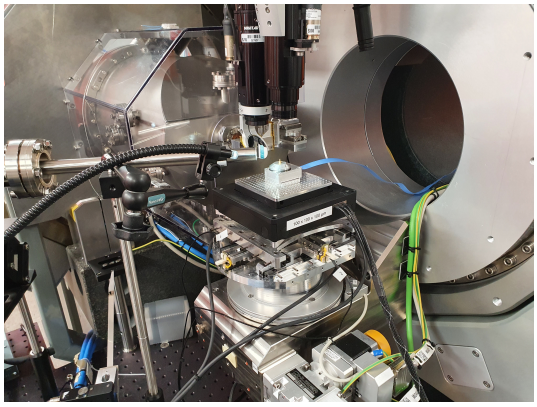

Figure 5: Sample position stage and scanner on top of the goniometer.

behind the goniometer frame can manipulate its position. Due to the high friction on the contact surfaces between the legs and the frame, the reproducibility is rather poor. However, in daily operation, only small adjustments are needed and are mostly within the adjustment range of the mirrors for the focal plane along the beam direction. For small lateral corrections, the KB chamber can be slightly moved.

The sample positioning stage on top of the goniometer rotations has been designed in-house. Commercially available stages were either lacking precision or stiffness, or did not fit in the available space. Rather than stacking each motion direction in individual stages, the sample stage has a fully integrated and compact design. The vertical axis is placed in the free space between the guides of the two horizontal motions. The travel range in the horizontal directions is 20 mm and in vertical direction 16 mm The axes are driven by high-force slip-stick piezos (PiezoLEGS LT40) and are operated in closed loop via a step-direction driver and the standard MAX IV motion controller (IcePAP).

The xyz sample scanner (nPoint NPXY100Z100-135) with a scan range of $100 \times 100 \times 100\,\mu m^3$ is mounted on top of the sample stage. A section of the vertical axis fits in the clear aperture of the sample scanner. The scanner and the sample stage can carry a payload of max. 1 kg. The sample scanner is driven by a digital piezo controller (nPoint LC.400). The controller outputs the position of the capacity sensors of the scanner as AquadB signals. During a flyscan this encoder output is then recorded by a PandAbox [3]. The PandaBox triggers also the detectors at each scan point of the flyscan. Flyscanning currently works on linear ramps with an acceleration and a deceleration phase, but the LC.400 controller allows the programming of arbitrary trajectories of all three axes, so that more flexible flyscanning schemes, such as spiral scans, can be implemented in the future.

1.5 Sample environments

The sample area of the diffraction endstation was designed to host a large variety of sample environments. The majority of experiments are run with isolated samples in air, using one of two types of standard sample holders. These are often shipped to users for sample mounting in the home lab. For special sample mounting or in-situ measurements, however, the endstation can fit customized sample environments. Figure 8 shows a selection of such environments that have been developed in-house, in collaboration with user groups, or for specific user experiments.

The electrochemistry cell in Figure 8a was developed in-house for in-situ coherent diffrac-

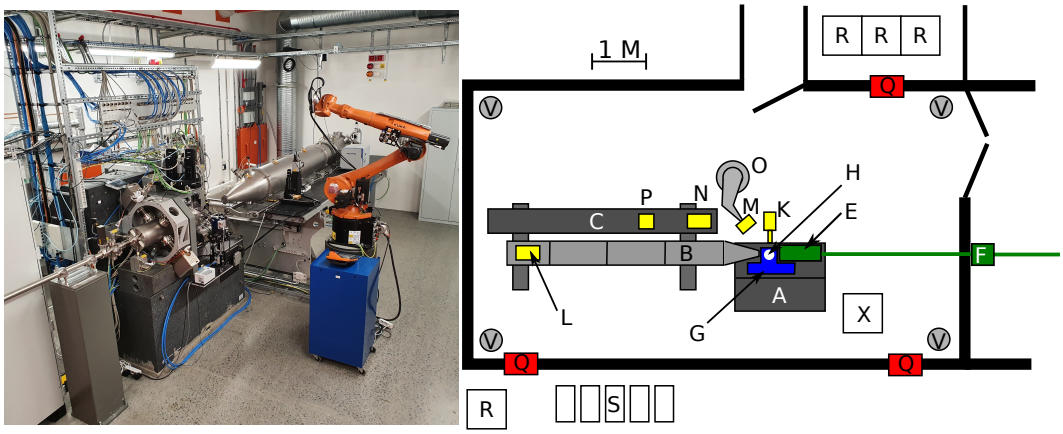

Figure 6: Left: Photo of the diffraction endstation with the detector robot and the vacuum flight tube. Right: Top view of the diffraction endstation hutch. A: Granite support, B: Detector vacuum flight tube, C: Breadboard for detectors and equipment, E: KB-optics chamber, F: Radiation safety shutter, G: Goniometer, H: Sample position, K: Fluorescence detector, L: Eiger detector, M: Merlin detector, N: Pilatus detector, O: Detector robot, P: Crytur detector, Q: Chicanes, R: Electronics cabinets, S: Pumps, chillers, etc., V: Ventilation exhaust. Ventilation inlet is trough the hutch ceiling (not shown).

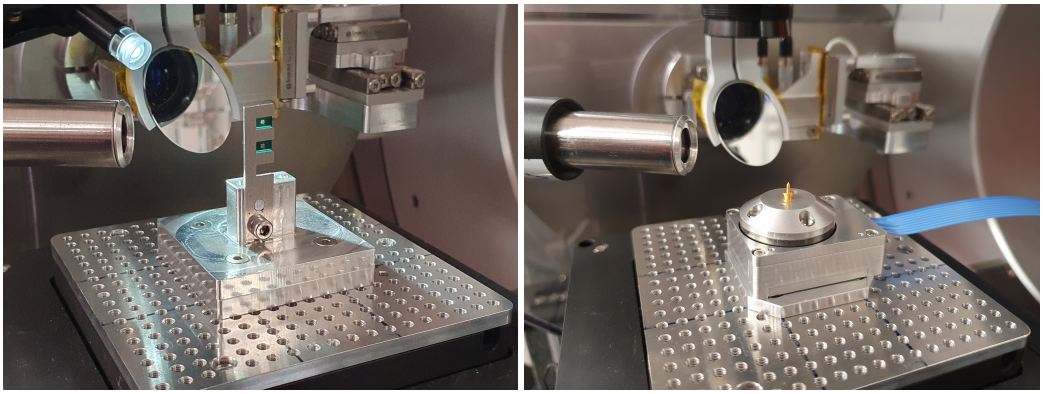

Figure 7: Images of samples mounted at the focal position. Left: Two Si3N4 windows with biological samples mounted on a standard sample holder. Right: A miniature rotary stage used for tomography measurements. The sample is mounted on a point-shaped sample pin, adapted from [4].

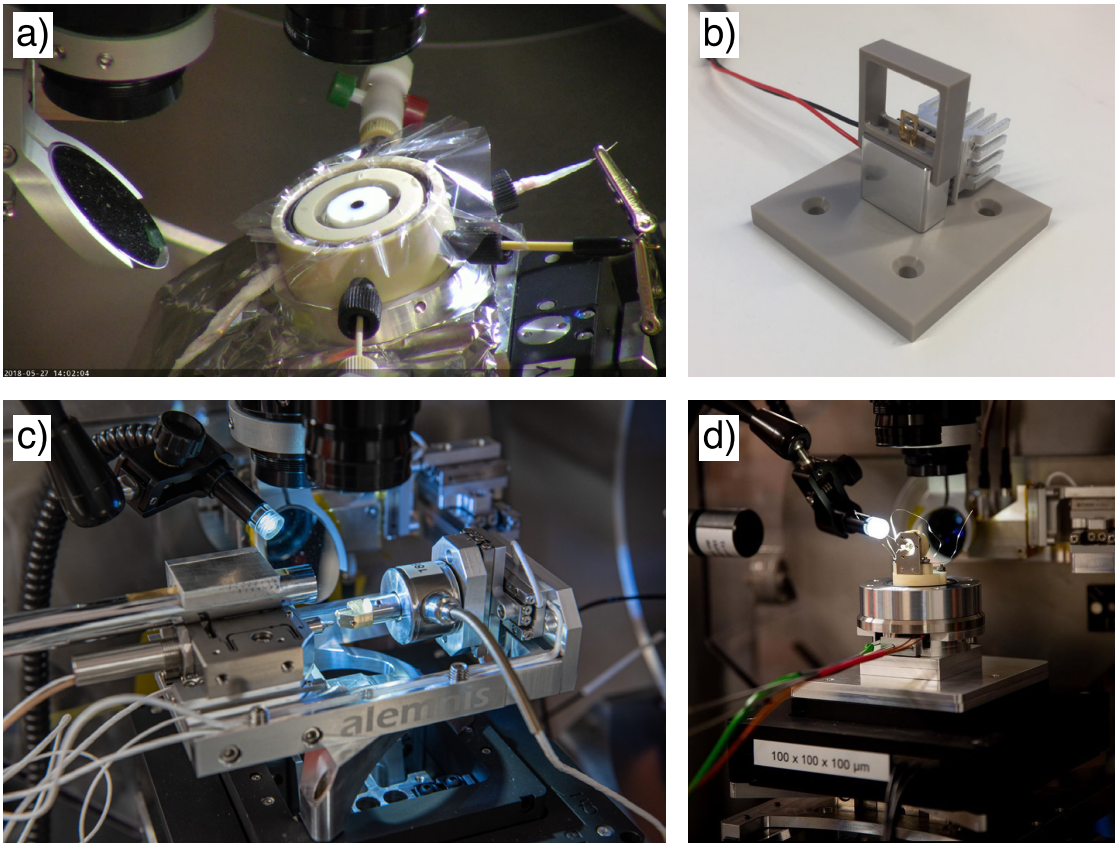

Figure 8: Examples of sample environments at the diffraction endstation: a) electrochemistry cell (in-house) b) moderate sample cooling (user experiment) c) in-situ nanomechanical testing (in collaboration with Magnus Hörnqvist Colliander, Chalmers University) d) sample heater with removed windows (provided by J. Wallentin, Lund University)

tion of nanoparticles under under electrochemical control by a potentiostat (Stanford Research Systems EC301) [5]. It contains a glassy carbon working electrode (3 mm diameter), a compact Ag/AgCl reference electrode and a Pt wire counter electrode. The window is made of 2.5 µm thick Mylar.

Figure 8b shows a sample holder for moderate cooling, that was developed for a user experiment. The holder kept Ikaite crystals in the sample below the phase transition temperature (7 °C). It used a Peltier element for cooling and a miniature thermocouple for temperature monitoring, that was attached directly to the sample holder. A small cover made of 2.5 µm thick Mylar foil reduced the condensation on the sample. A PEEK base plate decoupled the holder from the sample scanner and increased the thermal insulation.

In-situ nano-mechanical testing (Figure 8c has been implemented in collaboration with Magnus Hörnqvist Colliander from Chalmers University of Technology, and is now available to general users. It is based on a commercial nanoindenter by Alemnis, Swizerland, that operates in true-displacement mode. It is designed for dual use in an SEM and at NanoMAX. The sample, typically a TEM lamella prepared by FIB, is scanned in WAXS geometry repeatedly under increasing load of the diamond tip of the nanoindenter. Such series of scans take several hours and rely on the reproducibility of the scan positions. The nanoindenter experiments have suffered from the drift of the KB focus in the past, see 1.7.

A compact sample heater (Figure 8d) has been developed by J. Wallentin, Lund University, for the use at NanoMAX [6]. It can heat samples with a diameter of up to 7 mm to a maximum temperature of 500 °C in a controlled gas atmosphere at ambient pressure. The heater control is integrated in the beamline control software.

1.6 Beamline characterization

The beam at the diffraction endstation has been well described with a variety of methods. From a user perspective, the properties of interest are (i) the size and shape of the nano-focused spot, (ii) the coherence characteristics, and (iii) the intensity of a partially coherent but still nano-focused beam. These properties are all functions of photon energy.

A first beam characterization was done with a one-dimensional wave guide [7]. The wave guide serves as an ultra-narrow analyzer slit, and was used in a vertical orientation to characterize the KB focus along the horizontal direction. This method is very direct, and does not require resolution charts, pixel detectors, or phase retrieval software. By direct intensity measurement, the width of the focal spot was found to be close to the theoretical expectation for diffraction-limited focusing in the relevant geometry at 14 keV. Also, a high degree of coherence was found by measuring the visibility of Airy-like fringes in the focal plane.

A more detailed description of the beam can be obtained by phase-retrieval of a ptychographic dataset [10]. This method yields the phase and amplitude of the beam in an arbitrary sample plane, information which can be propagated along the optical axis to derive a full three-dimensional intensity profile. While essential for analysis of astigmatism of the beam during KB mirror tuning, this method can also give the detailed spot profile as function of energy. Figure 9A shows this energy dependence.

The ptychographic technique can also be used to describe the partial coherence aspects of the beam. By accounting for multiple probes and their mutually incoherent addition in the detector plane, orthogonal coherent modes are obtained [11]. This allows an analysis of the absolute and relative power in the first mode, compared to the others. Figure 9B shows such an analysis for a beam energy of 10 keV, and similar analyses were carried out as function of energy [8]. From this data, the coherent tuning curve in Figure 9C emerges, where a peak flux at 8 keV is seen, at $6 \cdot 10^{10}$ and $2 \cdot 10^{11}$ photons per second for a fully coherent beam and the first coherent mode,

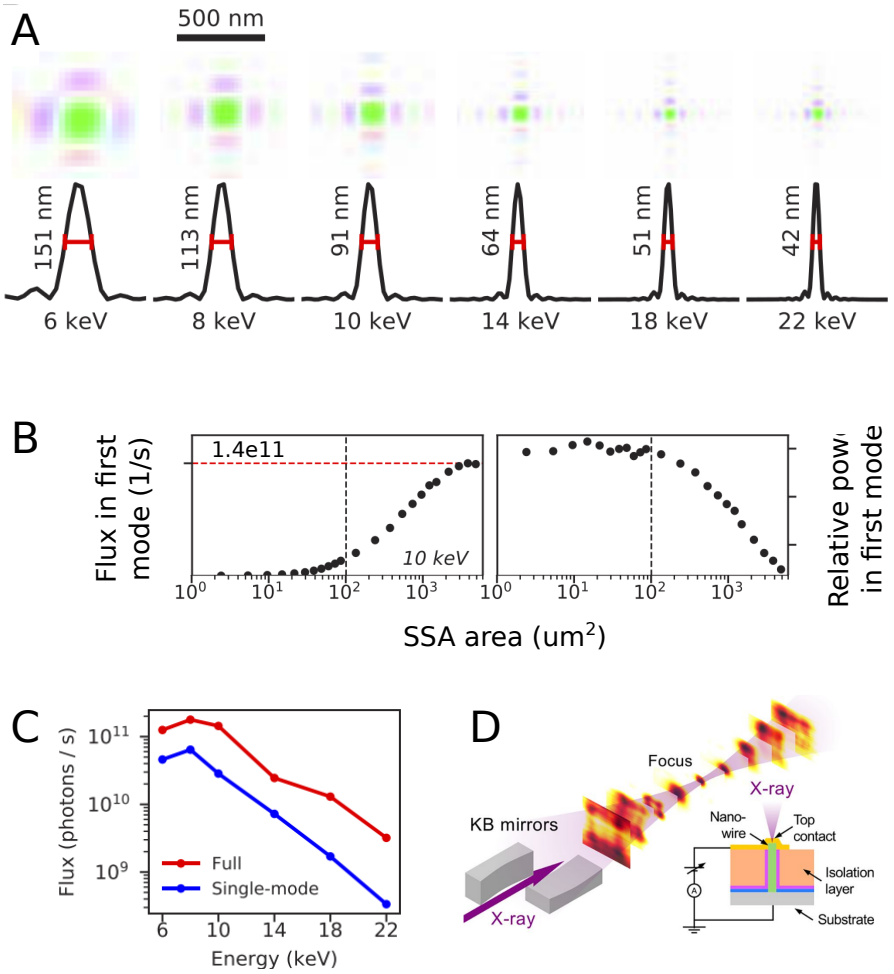

Figure 9: Beam characterization. A) Focal spot shape and width as function of energy, as determined via ptychography and beam propagation. B) Multi-mode analysis of the 10 keV as function of the SSA area. On the left, the first coherent mode can be seen to saturate at $1.4 \cdot 10^{11}$ photons per second, and on the right, the whole beam is seen to appear coherent up to an SSA gap of around 100 µm at this energy. C) Flux of a fully coherent beam together with the saturating flux of the first mode, often referred to as the *coherent flux*. D) Focal spot shape and near-field profile directly confirmed by using a single 60 nm wire as analyzer. Panels A-C are adapted from [8], and panel D comes from [9].

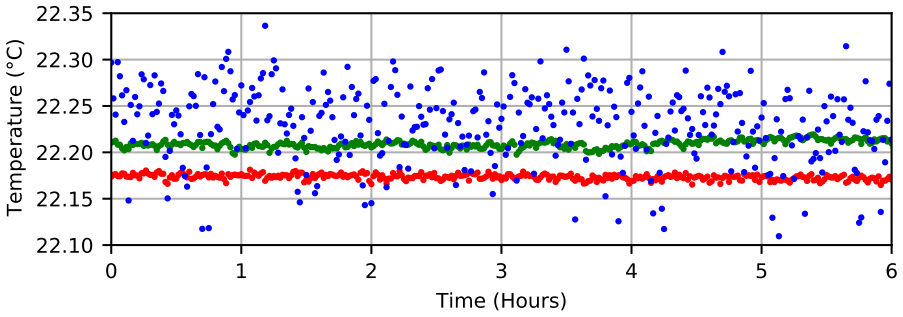

Figure 10: Temperature measured in the diffraction endstation hutch under static conditions for six hours. Temperature on sample (blue), on KB-vacuum chamber (green), on granite (red). Temperature fluctuates more on the sample than on heavier components. $2\sigma-$deviations for respective temperature are 83 mK (sample), 9 mK (chamber) and 8 mK (granite).

respectively.

The beam was later characterized in three dimensions directly with a scanning analyzer. In an impressive feat of nano-fabrication, a recurring user beamline user group managed to produce a p-i-n-doped single nanowire diode, vertically contacted to allow X-ray illumination along the wire axis [9]. The photocurrent was then recorded while scanning the device through the beam at and around the focus. The results confirmed the near-field diffraction patterns close to the KB focus, as shown in Figure 9D.

1.7 Stability

1.7.1 Thermal design and performance

The beamline infrastructure such as the floor, hutches, ventilation and water system were designed with care to minimize mechanical vibration, acoustic noise, cultural noise and thermal drift. To this end, the first optics hutch is constructed from steel and lead, and temperature-controlled to better than 0.5 K with recirculating ventilation. The two experimental hutches are built from concrete with a thermal insulation sandwich, where air between the hutch walls and roof towards the surrounding rooms increases thermal stability. Each experimental hutch has a recirculating ventilation system with large area air inlets in the ceiling and air outlets at the floor level. This design aims at providing a slow, laminar downward air flow resulting in thermal stability within 0.1 K at the sample position over weeks. Figure 10 shows temperatures measured at three positions in the vicinity of the sample over 6 hours during which the experimental hutch was closed. The sample temperature varies most due to the low mass of the used aluminium sample stick while the KB-optics chamber and the granite support are stable to within a few mK. All temperature fluctuations are, however, well below the design goal of 0.1 K. Upon entering the hutch, it can take a few hours regain stable condition after closure. To minimize thermal drift from active heat sources, most electronics are located outside of the hutch in designated rooms. Electronics that must remain close to the experiment, for example piezo controllers, electrometers and detector processors, are housed in a separately isolated ventilated rack close to the experimental setup.

The floor for the 3 GeV storage ring and all its beamlines is cast to become one unit [12]. This is to create one foundation with low vibration amplitudes due to its mass, where components close by on the floor are moving coherently. A cross-section of the floor construction is illustrated

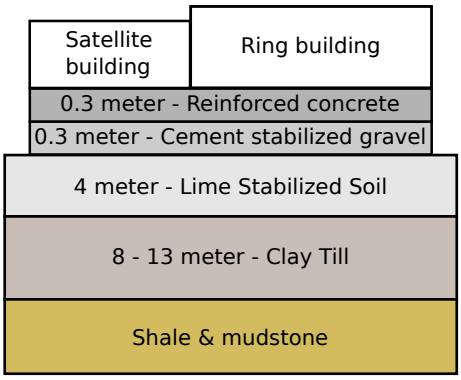

Figure 11: Foundation for the MAX IV buildings including the NanoMAX satellite house.

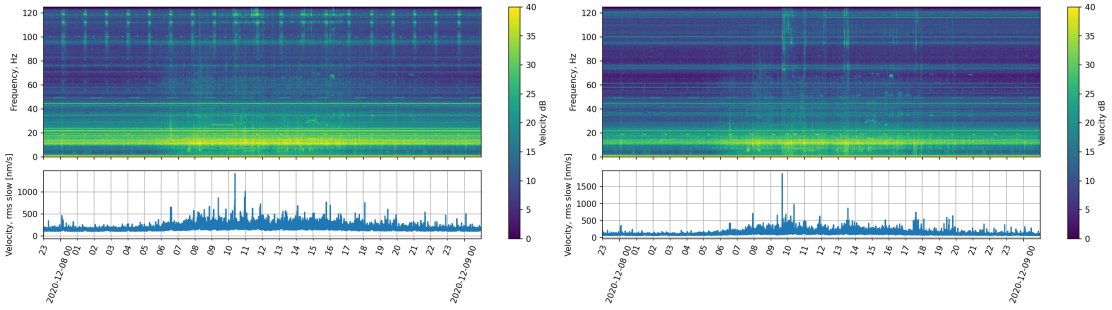

Figure 12: Seismometer spectra on a random working day. left: control room, right: experimental hutch.

in Figure 11. The MAX IV site is located on clay soil which was compressed during the ice age. Four meters of the ground is reinforced by a mixture of soil and chalk to make a stiff base. 300 mm of cement stabilized gravel and finally 300 mm reinforced concrete are cast to form the floor. All optical components are mounted on granite blocks, which are grouted to the floor. Equipment generating vibrations, such as vacuum pumps and chillers are suspended on tuned springs to reduce vibration transmission to the floor.

1.7.2 Ambient and sample vibrations

In an effort to identify external sources of vibrations, two seismometers are placed at NanoMAX. One is placed in the first control room. The second one records the floor vibrations inside the experimental hutch close to the diffraction endstation. The seismometer spectra are constantly acquired and archived. Figure 12 shows the spectrum of the floor vibrations over time on a random working day. Certain frequencies occur periodically. One of the sources was identified as a cooling unit in a rack room in the first control room. The other periodic sources have not been identified yet. In an ongoing effort with the Stability-Alignment-Metrology group of MAX IV, potential sources like transformer stations or ground water pumps have been ruled out.

Figure 13 shows the results of a stability characterization of the KB focus at the diffraction endstation with a diamond beam position monitor (DBPM). The DBPM is a position sensitive detector with 2 µm spacing between its quadrants. When the center of the void cross is placed in

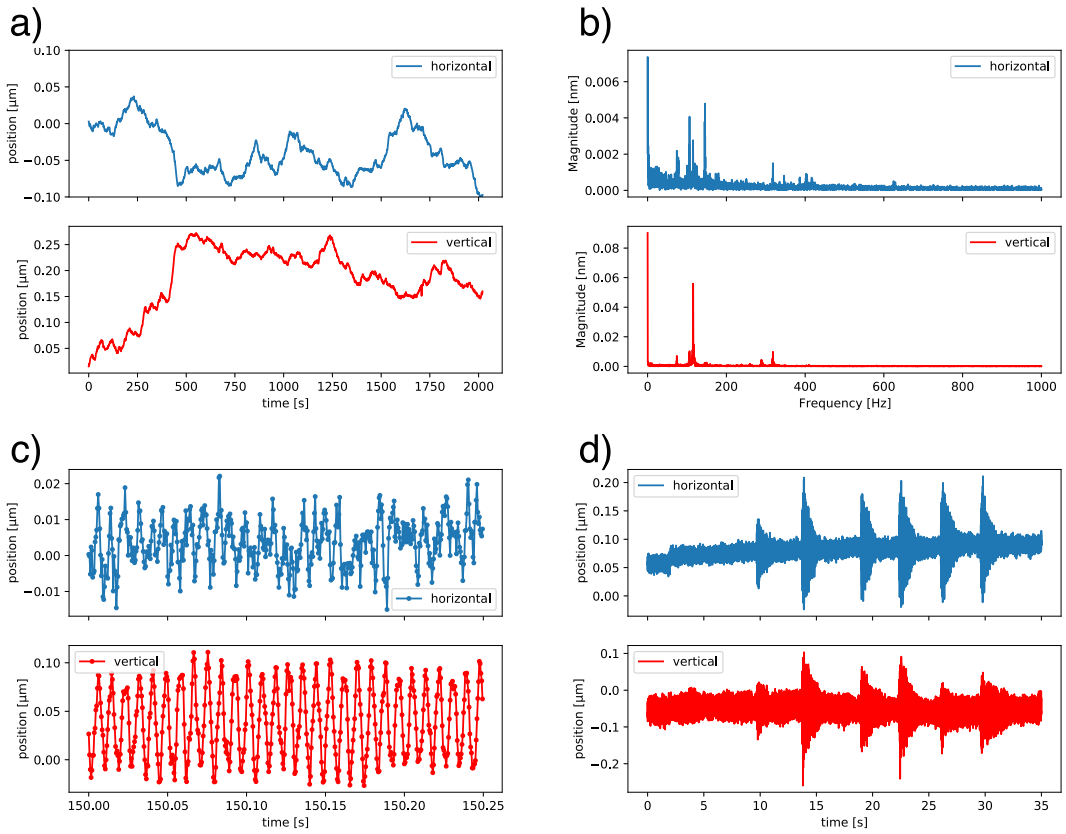

Figure 13: a) Horizontal and vertical beam motion over time after hutch access. b) frequency spectrum of the beam positions c) beam motion on short time scale d) beam motion after knocking (6x) on exterior building wall.

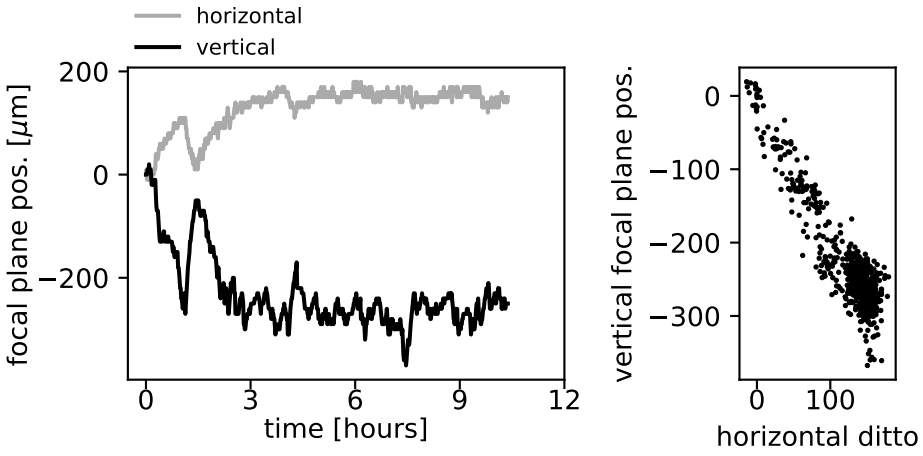

Figure 14: Left: The positions of the focal planes of the two mirrors during a 11 hour experiment, determined by numerical propagation of probes retrieved from 700 ptychographic scans. Right: The vertical and horizontal focal plane positions are correlated.

the KB focus, the response of the DBPM is sensitive to very small beam motions [13]. Thus, this setup allows the characterization of the relative motion between the DBPM on the sample stages and the X-ray focus. Figure 13a) shows the beam motion over a period of approx. 30 minutes after a hutch access. The beam position drifts over the whole period by up to 300 nm. The drift in the vertical direction is more pronounced. On a short time scale, the X-ray focus oscillates with an amplitude that is on the same length scale as the focus diameter, see Figure 13c). In the frequency spectrum of the DBPM positions (Figure 13b), several distinct resonance frequencies are excited. Figure 13d) shows the position response when the exterior wall of the control room is knocked six times, showing the susceptibility of the diffraction instrument to external excitation. The outdoor area around the satellite building is blocked for traffic during user operation to further reduce external vibrations.

1.7.3 Focal plane stability

The focal planes of the two KB mirrors are sensitive to the mirror pitch angles. Piezo actuators are used to fine-tune these pitches. In round numbers, a 1 µm linear displacement of each piezo causes the focal plane to shift by 1 mm along the beam. Therefore, the beam quality is sensitive to temperature variation and other sources of mechanical drift.

Experience has shown that the KB focusing is often stable for many days after settling. Other times, when the temperature of the hutch is assumed to drift, the focusing degrades faster. Figure 14 illustrates the settling of the two focal planes followed by fluctuations around a stable mean. To determine the focal plane positions, repeated ptychography was run during an 11 hour period after closing the hutch door. For each scan, the retrieved probe was propagated numerically to determine the two focal planes.

The settling data in Figure 14 shows considerable correlations in the two focal planes. This indicates thermal movement of the entire KB chamber, and a new mounting system for the chamber has therefore been designed. The upgrade will be installed during 2021.

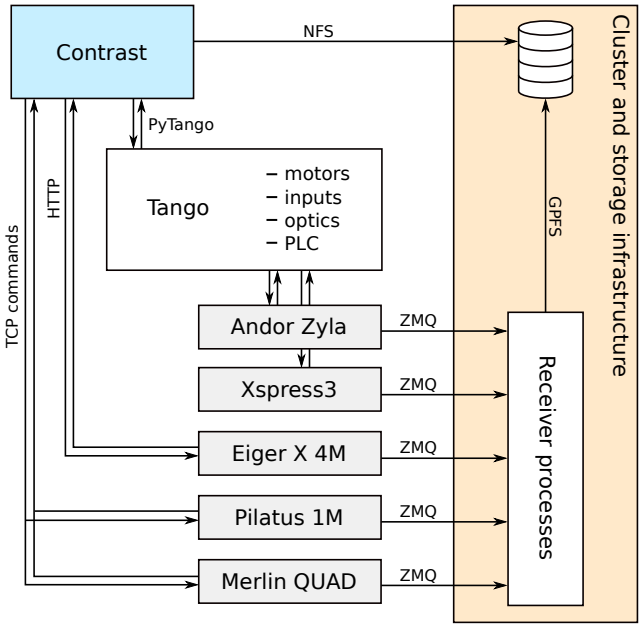

Figure 15: A summary of the beamline-driven, home-made control and acquisition system, together with streamed detector data pipelines [15, 14]

1.8 Control system development

During the first years of operation (2016 to mid-2019), the beamline was seriously impaired by an unstable control system. Aside from high software overheads, user experiments fell short because of constant software and server crashes. Extensive work was invested in improving the existing system, in close collaboration with the beamline's associated software engineer and the larger controls and IT group. Unfortunately, the situation was not resolved in an adequate way.

During 2019, a beamline-driven small-scale acquisition software named Contrast was therefore developed [14, 15]. The idea was to make a minimal, efficient, and flexible framework to improve the situation at NanoMAX. Its development is done within the beamline team, making sure that experimental realities and scientists' wishes are given priority. The system was deployed for user operation in September 2019 and has remained in place.

In parallel, streaming detector data pipelines have been developed, some of them with NanoMAX staff, which have increased the reliability and the achievable data rates from the pixel and array detectors. Contrast works well together with these data pipelines as summarized in Figure 15.

2 Transition to Operation

2.1 Brief history of user operation: calls and numbers

Formal user operation started very soon after the diffraction endstation was taken in use and the first focused beam had been produced. In 2017, four selected experiments were carried out, of which two were XRF mapping, one was scanning WAXS, and one was scanning diffraction of single nanocrystals.

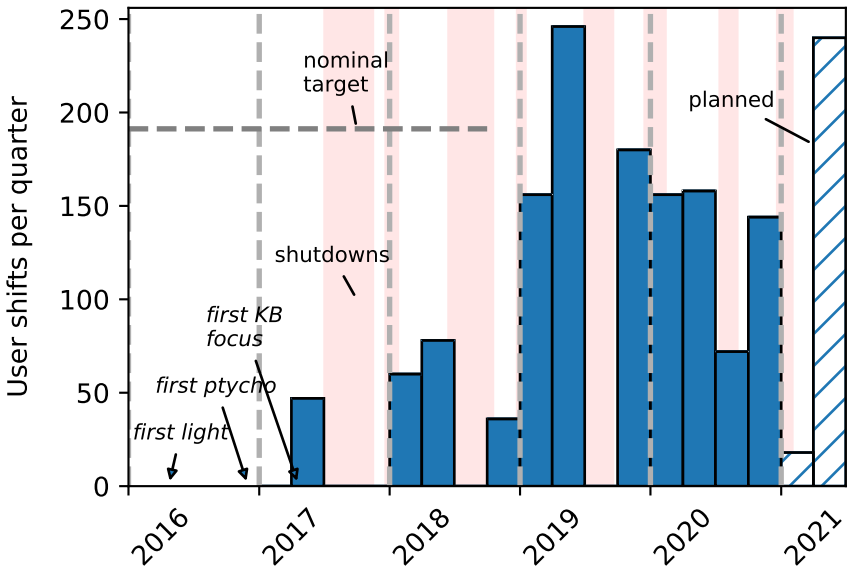

Figure 16: User operation statistics, showing the shifts actually carried out. The nominal target corresponds to 75 % of the available stored beam. The decrease in delivered shifts in 2020 was caused by the Covid pandemic. Data gathered Dec 2020.

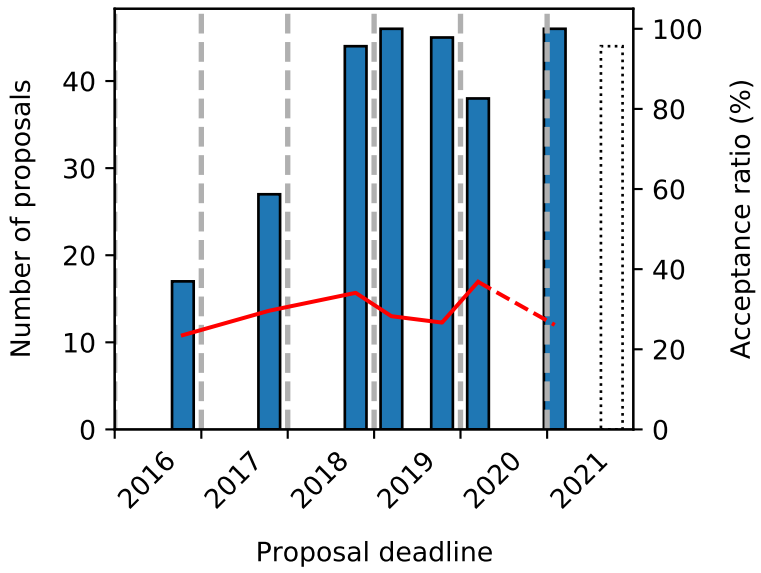

Figure 17: Number of received proposals for each call (bars), together with the acceptance rate (red line). These numbers reflect the committee decision, not the experiments actually carried out. Bar in dotted lined marks the next proposal call, in October 2021.

Figure 16 shows how the number of beam hours delivered to users has been increasing since. While 2018 saw the completion of many parts of the instrument, the number of hours delivered during 2019 reached 76% of the long-term target value (2328 out of 3060 hours). The beamline was scheduled to increase output further during 2020, but unfortunately the Covid pandemic caused massive cancellations. Reserve list experiments and follow-up experiments with local users were carried out where possible, but could not compensate for all the losses. The bars in Figure 16 show hours actually delivered. As of April 2021, the beamline is again allowed to open for remote user experiments, with full operation planned to return in September 2021.

Figure 16 also shows the machine shutdown periods as red vertical bands. As the synchrotron has approached a stable rhythm of planned shutdowns twice a year, the amount of total available beamtime has increased: currently, after deduction of a start up week and variable amounts of proprietary and educational time, the remainder is divided into 75% PAC-allocated user time, and 25% in house time (encompassing maintenance, commissioning and in-house research). A twice-yearly proposal cycle has also been adopted, with a current exception caused by the pandemic.

A high oversubscription rate has been maintained since user operation started. Figure 17 shows the number of incoming proposals per call, together with the fraction of proposals granted beamtime by the Proposal Advisory Committee (PAC). The absolute number of proposals has consistently been in the range 40-50 since beamline operations were ramped up. The pandemic has disrupted the twice-yearly call cycle, and it is not trivial to compare yearly proposal numbers when the number of calls varies. However, a saturation or slight decline is not unexpected after 2019, as the facility's novelty coincided with a long shutdown of the ESRF. We deem current levels of incoming proposals desirable on the long term, as reaching the target level of beamtime delivery would result in an acceptance ratio of around 40%.

2.2 Experimental techniques offered

NanoMAX offers a relatively wide range of different and often complementary X-ray techniques. These could be divided into two groups depending on whether they exploit and rely more on the beamline's nano-focusing capabilities or its unprecedentedly high coherent flux.

2.2.1 Nanoprobe techniques

The resolution which many scanning X-ray microscopy techniques can achieve is directly determined by the size of the scanning beam. When measuring samples in focus, NanoMAX achieves beam sizes in the range $40-200\,\mathrm{nm}$ – depending on beam energy – which enables high-resolution multimodal imaging with a combination of detectors and geometries.

Combining a 2D scan with a forward area detector (i.e. along the direction of the incoming beam) produces scanning transmission X-ray microscopy (STXM) data, generating transmission and differential phase-contrast images of the scanned areas which depend on variations of electron density and convey morphological information. Furthermore, wide angle X-ray scattering (WAXS) measurements can be carried out by positioning the forward detector as close as possible (ca. $150\,\mathrm{mm}$) to a sample with some degree of crystallinity.

In the Bragg geometry an area detector is positioned at a Bragg angle with respect to a crystalline sample and is used to collect X-ray diffraction (XRD) data which convey information on its lattice structure and cell. Scanning X-ray diffraction (SXRD) experiments are then achieved by scanning the nano-focused beam onto the sample.

Finally, a fluorescence detector is used within X-ray fluorescence (XRF) experiments which rely on atomic characteristic emission lines to generate elemental distribution maps and hence convey chemical information on the scanned areas. A fluorescence detector is positioned as close

as possible (ca. 15 mm) to the sample in order to maximise the detected solid angle and minimise air-induced signal pollution. Within NanoMAX's achievable energy range (5-28 keV) and exploiting both K and L lines, most elements with Z $\geq$ 15 can be detected – though quantification for low Z elements is hindered by air.

As they rely on different detectors and geometries, different scanning nanoprobe techniques can be combined. At NanoMAX, SXRD or STXM scans and XRF scans are typically performed simultaneously, producing multimodal images with the same focus-dependent pixel size.

2.2.2 Coherent techniques

Being a 4^{th} generation synchrotron radiation source, MAX IV offers an inherently highly coherent flux. Being a long beamline, NanoMAX further capitalises on this, enabling coherent X-ray imaging experiments to be performed with an unprecedented photon flux which in turn increases the achievable resolution. Coherent diffraction imaging (CDI) on samples smaller than the beam size and ptychography on extended samples both benefit from this. These are techniques which exploit coherent photons and geometric constraints to iteratively retrieve the lost phase information relative to the imaged samples. Their achievable resolution depends on reciprocal space sampling and is related to signal intensity at high spatial frequencies as well as detector's specifications and distance from sample. On the other hand, resolution is more loosely affected by beam size and ptychography experiments typically benefit of shorter acquisition times when using larger beams, without significantly compromising the achievable resolution. Also CDI experiments benefit from larger beams, as these allow for larger samples to be imaged. Therefore both ptychography and CDI experiments often make use of defocused beams.

In the Bragg geometry, both CDI and ptychography are carried out by measuring the diffracted signal – similarly to XRD – for different sample orientations, typically by performing rocking curves around a 2θ diffraction peak. The retrieved 3D phase conveys information on crystallographic strain and defects (e.g. dislocations). An alternative to Bragg ptychography is Bragg projection ptychography (BPP) which, in principle, enables 3D reconstruction even from single-angle 2D scans. This last approach has yet to be demonstrated at NanoMAX.

In the forward geometry, ptychography relies on far-field diffraction patterns to reconstruct the 2D complex-valued transmission function of the illuminated sample. This provides quantitative absorption and phase contrast and can successfully reconstruct even weakly scattering samples. Collecting projections at different sample orientations enables tomography and hence high-resolution 3D coherent imaging. Ptychographic X-ray computed tomography (PXCT) at NanoMAX has been recently demonstrated [16] and is currently offered to users (Section 3.4.4).

2.3 User support in practice

NanoMAX experiments are assigned local contacts at the time of scheduling. That way, technical planning can start months in advance. The team shares local contact duties evenly, and while each team member's special interests and skills affect assignments, most experiments can be supported by any member of the beamline staff. NanoMAX beamline staff comprises 4 permanent members (3 beamline scientists, 1 instrumentation scientist) and 1 postdoc. Further staffing requires external funding, outlined below in 3.5.

During the experiment, the local contact is on call to ensure extended user support. This service is available weekdays 8-23 and weekends 8-20. During on-call hours, the local contact is available by phone and has access to remote connections for solving smaller experimental problems. The local contact is also expected to quickly make their way to the beamline if needed.

Most users can autonomously run and evaluate their experiment after the first 1-2 days. After that, support is typically only needed for troubleshooting, realignment, extended data analysis, or for adding new elements to the experiment.

During the pandemic, some experiments have been carried out as remote mail-in experiments. This has relied on the local contact performing the measurements, and doing the first data evaluation. While remote desktop is available for staff, there is no proper remote access for users. Weekly changing set-ups also make the implementation cumbersome from a safety perspective.

2.4 Online data analysis

NanoMAX offers users several tools for online data analysis, both developed in-house and sourced from outside of MAX IV. User-oriented documentation is available on the beamline's wiki pages.

The graphical applications scanViewer and ptychoViewer are in-house-developed programs for simple visualisation of raw data and ptychographic reconstructions, respectively. ScanViewer is used for preliminary analysis and quick inspection of acquired data and enables simple manipulation to obtain 2D scan maps. It supports 2D detector frames (e.g. diffraction patterns) as well as 1D (e.g. fluorescence) and scalar data (e.g. ion chamber or diode readouts). It is typically used for wide overviews and test scans and especially for sample location and alignment. PtychoViewer is used to display ptychographically-reconstructed objects and probes, i.e. the transmission function of samples and the X-ray wavefront impinging on them. Knowledge of the complex-valued wavefront (i.e. probe) allows for numerical propagation which is also displayed in ptychoViewer in order to assess (and correct for) focal position and astigmatism.

Another set of scientific software is routinely applied both for online and offline analysis at NanoMAX. It includes Python-based packages, modules and libraries sourced from outside MAX IV. Each of them is technique-specific and available for free as maintained open-source code. The ones currently in use at NanoMAX include PtyPy, PyMca, PyNX and PyFAI.

PtyPy is an externally-develped and collaborately-maintained framework for ptychography [17]. At NanoMAX, simple ptychography scans on a well-known test pattern are typically used for beam characterisation and optics optimisation at least at the beginning of every experiment. Python templates are lightly edited (according to the experiment-specific parameters) and executed in PtyPy to perform fast ptychographic phase retrieval. This generates reconstructions of the complex-valued object and probe which are conveniently inspected via ptychoViewer. The suitability of the experimental and algorithm parameters is assessed by the agreement between the known test pattern and the reconstructed object. The reconstructed probe is then used to optimise upstream optics (e.g. KB mirrors).

PyMca is an ESRF-developed software for X-ray fluorescence (XRF) data analysis, including a rich graphical user interface [18]. It is used to display and fit XRF data as well as perform calibration (e.g. on known standards). It enables batch fitting on 2D scans, generates element-specific 2D fluorescence maps and allows for simple image manipulation.

PyNX is an ESRF-developed software for simulation and data analysis for coherent diffraction imaging (CDI) and ptychography [19]. At NanoMAX, it is used for the analysis of Bragg CDI (BCDI) data, i.e. CDI data collected in Bragg geometry.

PyFAI is an ESRF-developed software for fast azimuthal integration applied to X-ray diffraction data (XRD) [20]. At MAX IV, its graphical interface is used for calibration of XRD experimental setups based on Debye-Scherrer rings from reference samples. Such calibration is among the initial steps of experiments carried out in the wide-angle X-ray scattering (WAXS) geometry.

Both staff and users are able to use all these tools on a virtual desktop session on the NanoMAX compute cluster or use the JupyterLab-Interface provided inside the MAX IV network, although some familiarity with these environments is needed.

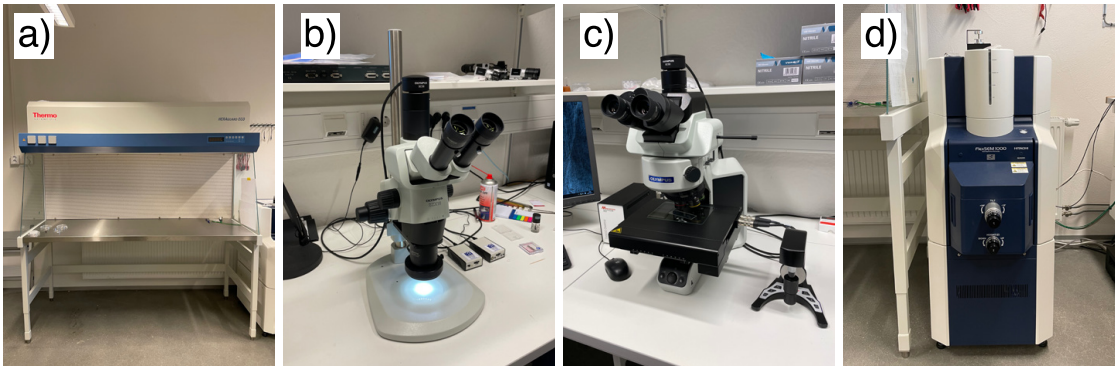

Figure 18: Equipment in the sample preparation lab at NanoMAX a) laminar air-flow bench b) stereo microscope (Olympus SX16) c) optical microscope with reflective and transmitted illumination (Olympus BX53) d) scanning electron microscope (Hitachi FlexSEM 1000).

2.5 Support Labs

NanoMAX offers several microscopes for the preparation and pre-characterization of samples in its sample preparation lab. Users can mount samples in a clean laminar airflow bench (Figure 18a). Samples can be mounted, inspected, and documented in a digital stereo microscope (Figure 18b). An optical microscope with reflective and transmitted illumination, bright field and dark field, DIC, polarized light, and a motorized sample stage can map and stitch large areas on samples at high resolution (Figure 18c). These sample maps are useful for navigation on the sample during X-ray measurements. A user friendly scanning electron microscope is also available to users (Figure 18d). The standard NanoMAX sample holders can be mounted in all available microscopes.

The preparation of biological samples for X-ray microscopy often requires adapted or special protocols. The Lund University Bioimaging Center (LBIC) has implemented such protocols and can assist in the sample preparation for X-ray microscopy, usually within the NanoSPAM framework (see 3.5).

The development and characterization of new setups is performed in the Nanomotion Lab at NanoMAX. On two optical tables, setups can be assembled and tested. It provides the same control software environments, so that developments can easily be transferred to the experimental stations. It offers the same thermal conditions as the experimental hutches.

3 Users, Science, Impact

3.1 Science strategy and target communities

From the start NanoMAX had two goals with its user operation program. The first is to make the most of the high-brilliance X-ray beam: enabling users to realize new science made possible by the facility's unprecedented coherent flux density and publish in high-impact journals. The second is to specifically engage with Swedish (and to a lesser extent Scandinavian) research communities. Here the motive is to strengthen Swedish research in general, via expanding a relatively modest nanoprobe user base to new groups and opening up research areas where synchrotron methods are not yet in common use. These aims don't necessarily overlap: maximizing on the coherence properties requires (extensive) synchrotron experience and favours users who can prepare, run

experiments and analyze data independently. On the other hand, taking on the wider Swedish research community shifts the balance towards more applied problems, which don't necessarily require methods that directly rely on coherence or beam brilliance (eg. scanning nano-diffraction, fluorescence mapping, XANES mapping, see section 2.2) and moreover may require a different level of user support. Beamtime allocation at NanoMAX aims at satisfying both goals.

That said, NanoMAX continues to receive high-quality proposals in a diverse set of research fields and for a wide range of X-ray nanoprobe methods. Therefore, as the PAC nominates proposals based on overall quality, a varied selection of experiments get carried out each proposal term. The beamline team does not directly define the science chosen, but works with both new and returning users, internationally and within Sweden, to attract, assist in writing and executing competitive proposals.

The external user groups can be crudely divided into a number of categories or scientific communities. First, a "functional materials" category can be identified, where users come with fabricated samples in the form of thin films or nano-structures. These groups are often interested in strain distribution, *operando* dynamics or auxiliary signals (e.g. current or polarization) and elemental distribution, and use both coherent imaging, nano-diffraction, and fluorescence. The samples can be pure semiconductors, assembled semiconductor devices, and ferroics of all kinds. A second category contains a diverse set of measurements of "biological samples", ranging from WAXS of tooth and bone samples, through high-resolution fluorescence mapping of thin tissue or plant sections, viral capsids and bacterial films, to the structural characterization of wood sections and paper samples. This collection of user groups is well represented both at Swedish universities, and even internationally, and have a diverse background in synchrotron experience. A third category is delineated by experiments on "polycrystalline materials" like soil, geological samples, steel and other engineered but disordered materials. Here, scanning diffraction or XRF is usually performed on natural or industrial bulk samples, prepared by polishing or FIB. These users typically belong to Swedish universities or industry, and have (often) a more limited experience of synchrotron methods and X-ray imaging. So far, experiments within the first of these areas have generated more publication output, likely because those researchers have often been experienced synchrotron users. Generally, users from the other two categories are more often inexperienced, and rely on heavy support during the experiment and, most importantly, in data analysis. Enabling inexperienced users remains one of the key scientific challenges for the beamline.

There is currently no intention to narrow down the range of methods offered to users, or the scientific communities with which to engage. Individual team members' own research interests do, however, gently modulate these engagements, and as in-house research and method development projects are very diverse (Section 3.4), beamline staff have co-proposed a variety of experiments together with the user community. The team's interests concentrate on applications where the nano-focused beam or its high degree of coherence are needed, to utilize the instrument's strengths, or towards enhancing the modalities of the beamline.

With the upcoming tomography endstation (see section 4.1) it is planned to distribute the already existing science cases and user groups to the two end stations according to the strengths and limitations of each endstation. For example the new planned capability of cryo- and in-vacuum sample mounting at the new tomography endstation will mostly benefit biological samples and materials, while any strain imaging or in-situ/operando measurements will still be best suited for the KB endstation. While the new endstation will likely attract new users, we mainly expect to keep and develop the existing user communities, but performing higher-quality experiments with the more specialized endstations.

Lastly, ideally, a micro-focus beamline at MAX IV would relieve NanoMAX and carry out pre-characterization or take on high-quality experiments which do not warrant a nano-focus.

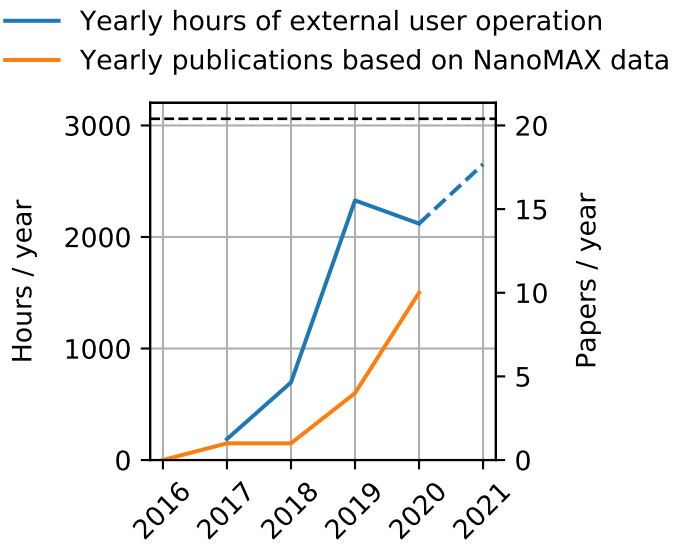

Figure 19: Yearly output in terms of hours in external operation as well as publications. The dashed line shows the nominal target for delivered user hours corresponding to 75% of the available stored beam. The decline in 2020 is a result of the Covid pandemic. Data gathered Dec 2020.

Until such an instrument is negotiated and built, the NanoMAX team strategically engages in projects that genuinely benefit from a (coherent) nanobeam, even if this commitment at times excludes engaging in potentially productive projects, in particular in applied research within Sweden.

3.2 Scientific production

With an explicit goal of 300 papers published across MAX IV annually, it is clear that expectations on NanoMAX to produce publications are high. As a flagship beamline which was among the first to come online at the facility, both the user operation and in-house research programs can now be expected to produce measurable output. Seen from the user operation perspective, the goal must be that some significant fraction of the 20-25 yearly external experiments result in published results. Together with in-house research and instrument development, 15-20 published papers per year appears a reasonable long-term expectation.

Figure 19 shows that the number of yearly publications is rising, and appears to lag behind the operation ramp-up by a year or two, as somewhat expected. While initial publications were typically technical and appeared in respectable but specialized journals, 2020 saw the acceptance of NanoMAX-derived papers in more prestigious science-focused outlets, such as *ACS Nano*, *Nano Letters*, and *Physical Review Letters*.

Table 4: List of publications based on NanoMAX data. An asterisk (*) marks groups based at Lund University and in-house research.

First author	Title	Journal	Group
2021 (April)			
Nukala	Reverible oxygen migration and phase transitions in hafnia-based ferroelectric devices	Science	Noheda
Tuukka	Ice-Templated Cellulose Nanofiber Filaments as a Reinforcement Material in Epoxy Composites	Nanomaterials	Oksman
2020			
Björling	Three-dimensional coherent Bragg imaging of rotating nanoparticles	Phys. Rev. Letters	in-house*
Chayanun	Direct 3D imaging of an X-ray nanofocus using a single 60 nm-diameter nanowire device	Nano Letters	Wallentin*
Kahnt	First ptychographic X-ray computed tomography experiment on the NanoMAX beamline	J. Appl. Cryst	in-house*
Marcal	In Situ Imaging of Ferroelastic Domain Dynamics in CsPbBr3 Perovskite Nanowires by Nanofocused Scanning X-Ray Diffraction	ACS Nano	Wallentin*
Barreto	Multiscale characterization of embryonic long bone mineralization in mice	Advanced Science	Isaksson*
Hammarberg	High resolution strain mapping of a single axially heterostructured nanowire using scanning X-ray diffraction	Nano Research	Wallentin*
Dzhigaev	Strain mapping inside an individual processed vertical nanowire transistor using scanning X-ray nanodiffraction	Nanoscale	Mikkelsen*
Ji	Crystallography of low Z material at ultrahigh pressure: Case study on solid hydrogen	MRE	Mao
Akan	Metal-Assisted Chemical Etching and Electroless Deposition for Fabrication of Hard X-ray Pd/Si Zone Plates	Micromachines	Vogt
Björling	Ptychographic characterization of a coherent nanofocused X-ray beam	Optics Express	in-house*
2019			
Björling	Coherent Bragg imaging of 60 nm Au nanoparticles under electrochemical control at the NanoMAX beamline	J. Synchrotron Rad.	in-house*
Chayanun	Combining Nanofocused X-Rays with Electrical Measurements at the NanoMAX Beamline	Crystals	Wallentin*
Osterhoff	Focus characterization of the NanoMAX Kirkpatrick–Baez mirror system	J. Synchrotron Rad.	Salditt
Griesmayer	Applications of Single-Crystal CVD Diamond XBPM Detectors With Nanometre X-ray Beams	13th Int. Conf. on Synchr. Rad. Instr.	CIVIDEC
2013-2018			
Johansson	Initial Operation of the NanoMAX Beamline at in-house*	Microsc. Microanal.	in-house*
Vogt	First x-ray nanoimaging experiments at NanoMAX	SPIE Proceedings	Vogt
Kristiansen	Vibrational performance of a cryocooled Horizontal DCM	J. Synchrotron Rad.	FMB Oxford
Johansson	NanoMAX: a hard x-ray nanoprobe beamline at MAX IV	SPIE Proceedings	in-house*

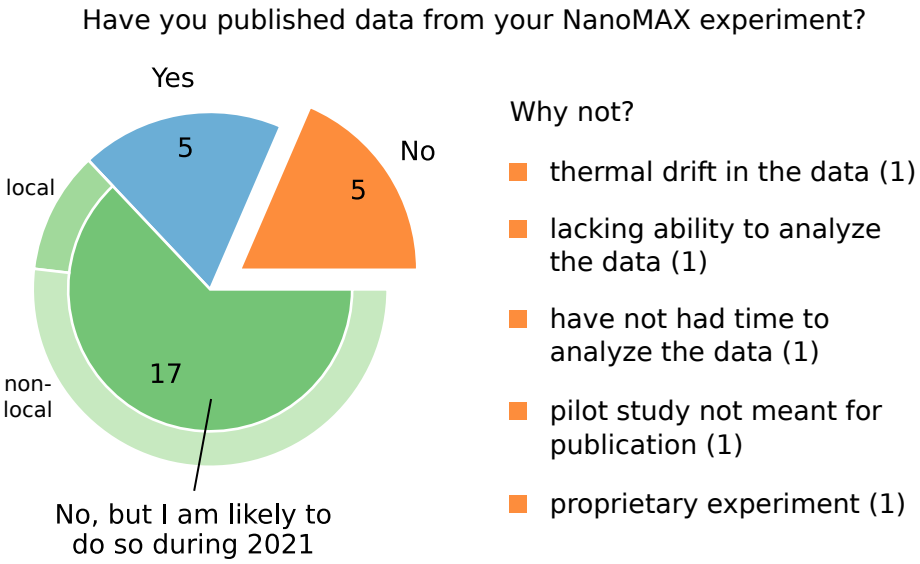

Figure 20: Answers from a questionnaire sent to the 43 user groups which visited 2018-2020. Most are optimistic about publishing their results within a year. The label ”local” refers users affiliated with MAX IV or Lund University.

Table 4 shows a full publication list (as of April 2021). While the increased output during 2020 is clear and convincing, looking into the research groups behind the papers shows a bias. Out of 10 publications, 3 reported on in-house research, 5 were written by groups at Lund University (most of them from the Wallentin group), one comes from the group of a beamline spokesperson at Stockholm University, and only one came from a completely external user group. This bias raises obvious concerns as to the productivity of external user operation. The table also reveals that no non-expert Swedish groups have published so far, and that with the exception of a paper from the Isaksson group, the XRF mapping experiments have not generated publications. There is a significant overlap with the non-expert group.

A questionnaire was sent to the 43 user groups that had visited the beamline during 2018, 2019, and 2020, with the aim of finding possible bottlenecks to publication. Emphasis was placed on scientific output and on possible obstacles to producing publishable results, with specific questions on beamline support, completeness of the data set and data analysis obstacles. Figure 20 shows answers to the specific questions on publication. Recognizing that the response rate at 63% was lower than desired and that responses are likely to be overly optimistic, it is still notable that the majority of responding users predict to be publishing their results within a year. A majority of these optimistic responses came from users not affiliated with Lund University or MAX IV, which is at least encouraging.

Unfortunately, the questionnaire did not identify any clear bottlenecks. Among the respondents who had not yet published and did not expect to do so this year, the five answers were disparate. Lacking ability and time to analyze data, along with low data quality were each given as reasons once. Based on interactions with users over the past years, it is the beamline team’s impression that a lacking ability and knowledge in data analysis remains the single largest bottleneck, at least in the group of Swedish external users who do not have extensive experience of synchrotron measurement and data analysis.

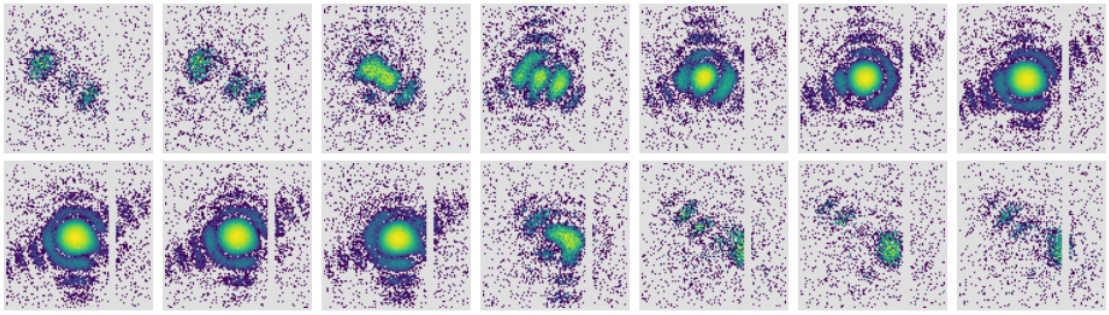

Figure 21: Selected frames from a time series, where the (111) coherent Bragg reflection is recorded as a 60 nm gold particle rotates under the beam.

3.3 User feedback

MAX IV uses a simple feedback system, where users fill in an end-of-run form in the digital user office system. They are asked to grade the quality of user support, facilities, control system etc. on a scale of 1-5 (high score better quality), and can give free text comments. Unfortunately, users tend to use only the top of the scale, resulting in an average between 4 and 5 for all questions. While this points towards an overall level of satisfaction, it makes the tool a bit too insensitive to extract real qualitative information. The written comments, however, give a better feeling for user satisfaction and also allow to see the development of the beamline. We include all user comments (no omissions) on beamline support, technical capabilities and improvement suggestions from the start of operation at NanoMAX in Appendix A.

3.4 In-house research and development

3.4.1 Single-particle BCDI

In recent years, Bragg Coherent Diffraction Imaging (BCDI) has started to become popular for the purpose of imaging working catalyst particles *in operando*. While penetrating power and strain sensitivity are huge benefits of X-ray imaging in this context, the endeavour is still questionable from a catalysis point of view. With a few exceptions, the particles imaged so far (200-500 nm) are still orders of magnitude larger than those used in real catalysts (2-10 nm), where surface-to-mass ratios are pushed to the limit. The strong scaling of signal with particle size ($I \propto d^4$) means that reaching realistic catalysts is at best a challenge.

An obvious application of the coherent flux density of NanoMAX is to push the state of the art in BCDI particle size. To this end, 60 nm gold particles were imaged inside an electrochemical cell, and the results published as an indication of where the limits of *operando* BCDI might lie [5]. This work is proceeding further with a planned electrochemical experiment before summer 2021.

The 2019 study showed clearly that particle stability becomes limiting as particles shrink and flux densities increase. Specifically, the X-ray beam caused the 60 nm gold particles to undergo spontaneous rocking curves, which could be filmed on the Bragg detector (Figure 21). A numerical scheme to assemble these sequences into coherent diffraction volumes, recovering the angular trajectories, was developed in collaboration with the Maia group at Uppsala University. The results were published recently [21] and show how the stability limit in BCDI can be circumvented.

This line of in-house research will continue by (i) pushing the limits in particle size further and (ii) extracting actual surface-chemical information via experiments on various electrochemical

systems. Funding for a postdoctoral scholarship on this subject has been applied for.

3.4.2 Multimodal microscopy (*aka* efficient nanoXRF)

One common practical difficulty encountered while performing X-ray fluorescence (XRF) microscopy experiments at the nanoscale is that of reliably identifying regions of interest (ROI). Often this is done by performing coarse XRF scans with a relatively large step size and possibly a defocused beam in order to obtain overview maps of the sample. However this entails mainly two disadvantages. On the one hand, a pixel-by-pixel scanning technique is by nature time-consuming. On the other hand, relying solely on fluorescence emission could be sub-optimal in terms of photon usage, especially for organic or other light-element samples. In light of this, a more photon-efficient way of generating overview images has been implemented based on in-line holography. At NanoMAX, this has been achieved by extending the sample translation stage along the optical axis in order to access a wider range of defocusing distances (up to 46 mm) and adding a near-field sCMOS-based camera system to the standard XRF setup. The combination of optical magnification within the camera system with the magnifying effect of the divergent beam allows to produce images with a spatial resolution comparable to that achieved with XRF, yet with an imaging speed (i.e. imaged area per unit time) 2 orders of magnitude higher. This results not only in faster overview scans but also in more dose-efficient ones, with great benefit for radiation-sensitive (biological) samples. This approach in which fast overview images are generated via in-line holography, followed by longer nanoscale XRF scans has been demonstrated in-house within 2020 in close collaboration with other researchers from Lund University [22]. Beside dose- and time-efficiency, this 2-technique approach offers the advantage of generating images based on different and complementary contrast mechanisms: while XRF provides chemical information through elemental distribution, holography provides morphological information based on electron density. Finally, collaborative research continues for the establishment of holo-tomography which – independent of XRF measurements – would provide 3D information from weakly scattering samples at the mesoscale (i.e. with spatial resolution within the range 100 nm to 1 µm).

3.4.3 Spectral microscopy

An obvious advantage of an X-ray nano-focus achieved via achromatic focusing optics is that of being relatively stable to photon energy variations. This feature has been exploited within exploratory in-house research aimed at expanding NanoMAX's spectral capabilities. Unlike conventional X-ray absorption near-edge structure (XANES) spectroscopy experiments which are often aimed at characterising bulk samples, spectral microscopy allows only for far less invasive sample preparation as this could alter – if not destroy completely – relevant nanostructures. Therefore, even though sample thickness can be controlled to some degree, its inhomogeneity could be wide. And if this appeases the inquisitiveness of the microscopist, it can't but upset the spectroscopist. In practice, the sturdiest way to first approach the task has been via indirect XANES, i.e. based on fluorescence yield rather than attenuation. In 2020, spatially-resolved XANES has been carried out within pilot experiments: sets of indirect XANES data were obtained by collecting series of fluorescence maps with a focused beam at varying energies around an absorption K edge (e.g. Fe and As). Data quality was sufficient to reveal chemical shifts of the absorption edges although finer structures were hidden by noise. Another approach tested just when MAX IV was last freely accessible (Dec-2020) was based on spectral ptychography. In this case far-field ptychography scans with a defocused beam were repeated in forward geometry at varying photon energies. Retrieval of each attenuation map relied on the better contrast ensured by phase shift which proved particularly helpful in the case of weakly scattering samples.

Although for such samples – which entail low edge jumps – signal-to-noise ratio for attenuation-based XANES is inherently poorer than for fluorescence yield, spectral ptychography still offers the great advantage of a higher imaging speed: a defocused beam can in fact be scanned onto the sample to obtain images with spatial resolution smaller than the focal spot size. For both indirect XANES and spectral ptychography, data analysis was further complicated by distortions in single-energy images caused by instabilities within the experimental setup and possibly changes within the sample. Still, preliminary results are promising enough to encourage the pursuit of further research along this line. Fast spectral ptychography in particular will be carried out at the nanoscale at selected energies sufficient for determining chemical speciation of elements of interest based on reference samples.

3.4.4 Developments in ptychographic tomography

X-ray ptychographic computed tomography is offered at more and more synchrotrons around the world. MAX IV with its high coherent flux should be predestined for such a method, which is based on the coherent fraction of the provided beam. In December 2019 we proved that PXCT experiments are feasible at the NanoMAX beamline [16] and identified the most critical factors limiting the quality of the results. Even though the PXCT experiments at the diffraction endstation are based on a rather improvised setup, we could push the usability and quality within a year to a level that PXCT could be offered successfully to users. In December 2020, such PXCT experiments were even combined with the recording of XRF tomograms of the same sample regions. The data taking and automatic reconstruction of the recorded projections was stable enough to acquire full tomographic datasets without intervention (only supervision) of an operator (see section 4.3). It is planned that those types of experiments will eventually be performed at the more suited tomography endstation and only experiments requiring more freedom for sample environments will fall back to using the diffraction endstation.

With the increased routine in performing PXCT experiments it is planned to (i) use it for exciting experiments with science cases beyond the method, and (ii) push the development of the technique as a whole (and not just its implementation at the NanoMAX beamline). In-situ limited angle tomography experiments on the restructuring of industrially relevant catalytic systems have been proposed (by us) and accepted at NanoMAX. They have, however, not yet been performed, due to scheduling difficulties following the Covid pandemic. All necessary capabilities (except for the reactor provided by co-proposers) are however present at the beamline. It is intended to use PXCT data recorded at NanoMAX to further explore the capabilities of coupling the ptychographic reconstructions step with the tomographic reconstruction step. The recent addition of the in vacuum Eiger2X 4M detector and the motorized flight tube should allow to take high quality data, well suited for these new types of algorithms.

3.4.5 Real-time ptychography

In an effort to make ptychographic imaging both more efficient and more accessible to non-experts, a joint project with Uppsala University on real-time ptychographic reconstructions is being launched in May 2021. The project first aims at setting up the infrastructure and data logistics needed for real-time ptychographic reconstruction, with the objective to make ptychography as easy to use as any other scanning microscopy technique. Then, novel algorithms for reconstruction and making phase-retrieval parameter choices will be developed. This second part of the project will rely on the expertise of the Uppsala team in optimization and machine learning. A PhD student has been recruited, and will be supervised by Filipe Maia with a secondment to MAX IV.

3.4.6 FZP optics, test structure and novel instrument development

The tomography endstation, currently under development, will use FZP optics to reach 30 nm resolution. A program to develop the needed zone plates has been running at the Royal Institute of Technology (KTH) in Stockholm by the Vogt group, since the start of the beamline project. To develop the zone plates, a metal-assisted-chemical-etching (MACE) process has been used to create a zoneplate mold in Si where electroless deposition is used to metalize the structure with Pd[23]. The fabricated zone plates have a 1:1 line-to-space-ratio, 30 nm outermost zone width and an aspect ration of 30:1. The zone plate efficiency has been measured at NanoMAX in a temporary setup in the first experimental hutch. At 9 keV the efficiency was measured to 1.9 % at first order diffraction.A number of FZP:s are waiting to be used when the tomography station is ready for first tests. The Vogt group is also developing customized nano-fabricated structures used in optics characterization work at the beamline. Patterns such as Siemens stars, checker boards, and line arrays are made on a common wafer for efficient use.

NanoMAX is a partner in a project entitled *Stereoscopic X-Ray Vision to Investigate Nucleation, Growth and Assembly of Nanoparticles in 3D* together with the KTH group and scientists from P06 at PETRA III. The project is funded with a Röntgen Ångström grant and runs until the end of 2023. The main goal of the project is the in-situ investigation of nucleation and growth mechanisms of nanocrystals in solution with high spatial resolution. Since typical sample environments for these purposes are large, the aim is to develop a new stereoscopic X-ray imaging technique based on a combination of multi-beam and multi-slice ptychography to enhance the depth-resolution without the need to rotate the sample. A successful implementation will also require to further develop X-ray optics and build an ultrastable microscopy setup to achieve 3D hard X-ray imaging with highest possible spatial resolution. Testing of prototype instrumentation is planned to take place in the first experimental hutch at NanoMAX.

3.5 Support infrastructure

The NanoMAX beamline is part of the Imaging group, comprising NanoMAX, SoftiMAX, MAXPEEM and the offline microscopy lab (STM, AFM, SEM). It also has notable close contacts with CoSAXS, on coherence methods, and Balder, where the spectroscopy techniques complement imaging techniques at NanoMAX. Other MAX IV groups and departments are an obvious asset in supporting NanoMAX, with the sample environment and detector support group (SEDS), CAD engineers, and IT services as examples. MAX IV is a part of Lund University, which offers further possibilities for joint research and development projects, which is reflected also in the number of publications from local users. Moreover, a shared postdoc between the Department of Biomedical Engineering (Isaksson group) and NanoMAX is due to start in September 2021.

The university also hosts the Lund NanoLab (LNL), part of NanoLund; an interdisciplinary consortium of researchers focused on Nanoscience. At the LNL a suite of clean rooms and equipment is available for sample growth, treatment and characterisation through collaboration and training, or payment. Focused ion beam milling (FIB) in particular, has proved useful for tomography sample preparation at NanoMAX. It is thought that in the coming five years the LNL and the Synchrotron radiation department within Physics will relocate to Science Village, the area between ESS and MAX IV, for even closer proximity.

Another Lund-based initiative is LINXS, the Lund Institute of advanced neutron and X-ray science, which supports prospective (local) users in gaining knowledge and seeking access to ESS and MAX IV, and provides funding for organizing workshops and hosting science fellows, within periodically changing focused themes and work groups. At NanoMAX an early LINXS program brought David Paterson from the Australian synchrotron for a three month visit to set up early

XRF experiments in 2017. The current CoWork webinar series, bringing together researchers interested in coherence properties of X-rays, is also hosted by LINXS.

As a spin off from LINXS and a European Interreg project, national funding was obtained for a four year program (2019-2022) called NanoSPAM, facilitating access and sample preparation for users from a Life Science background to the Imaging beamlines at MAX IV. Biolabs in Umeå, Lund, Stockholm and Gothenburg, specialized in biosample preparation - such as (ultra)microtomy, plunge freezing and chemical fixation methods - form a bridging network between the beamlines and prospective users with a biological/biomedical question. In Lund, a dedicated person is employed (50%) within this program. This has solved the first hurdle for these users, who mostly apply to NanoMAX for XRF mapping. As a future development, we have seen that we have to focus more efforts on data analysis and help in understanding the X-ray techniques for their samples. The joint postdoc with Biomedical engineering is working towards a streamlined XRF experience as part of his beamline contribution tasks.

4 Future Directions

4.1 The tomography endstation

In contrast to the diffraction station's design to be configurable, the tomography endstation will be optimized for highest spatial resolution at the cost of flexibility. The detailed design work of the instrument is currently ongoing with the goal to manufacture and assemble core components during 2021. Figure 22 shows a snapshot of the mechanical design in April 2021. The instrument will be built to operate in vacuum and have liquid nitrogen cooling of the sample. Fresnel zone plates will be used for focusing down to 30 nm with a long-term goal to reach 10 nm. A three-axis piezo scanner and a rotary stage will allow two dimensional and computed tomographic imaging. A multi-element X-ray fluorescence Silicon drift detector will be used to acquire elemental information in two and three dimensions with extreme spatial resolution. A flight tube, similar to the one at the diffraction station, will house the existing Eiger area detector or a dedicated similar detector. The section of the flight tube with the detector is designed to be easily moved between the two endstations. Fibre interferometers will measure positions of both the sample and the FZP to reach the needed positional accuracy. Sample transfer will initially need venting of the chamber, and warming up if the sample was cooled. However, in a second development step, we aim at realizing a load-lock system to allow more convenient sample exchange. The microscope chamber and the flight tube will be designed to allow easy pass through of the photon beam to the diffraction station downstream. As discussed in section **??** anove, the tomography station will have similar capabilities as the OMNY instrument at cSAXS (SLS), ID16A (ESRF) and the BioNanoProbe (APS). However, these are extremely advanced instruments where considerable development efforts have been invested. We aim at developing, in some respects, a simpler instrument, possibly with a smaller feature set.

4.2 Developments at the diffraction station

With the transition to routine user operation several areas for further improvements of the diffraction endstation have been identified. One of the issues is the stability of the KB focus. Both the long-term stability and vibrational stability of the KB focus is affected by the stability of the mechanical support of KB mirror chamber. Long-term thermal drifts cause the chamber to move which changes the incidence angle on the KB mirrors slightly. This results in a lateral and longitudinal shift of the KB focus. Also, external vibration sources excite resonance frequencies in the KB chamber and the mirror mechanics. In an already started project the support of the

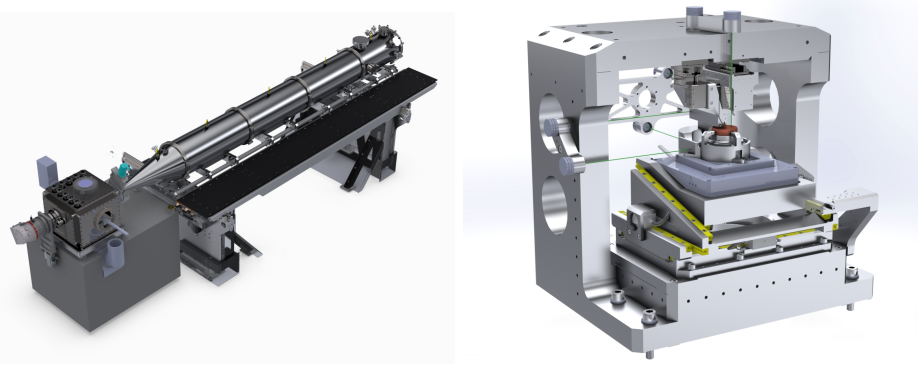

Figure 22: Model of the tomography endstation. Left: Overview with the microscope vacuum chamber on the support granite and the detector vacuum flight tube. Right: The interior parts of the microscope chamber. The sample scanner, rotation stage and positioning stages are seen in front. Above and behind are the optics alignment stages and interferometry mounted on the bridge structure.

KB chamber is redesigned. The motorized support is very rarely used for the alignment. Within the project, rigid, manually adjustable supports are explored.

If the stability improvements by a new chamber support is not satisfying, the whole concept of the KB mirror mechanics and the chamber support need to be reevaluated. Within that context, the overall design of the diffraction endstation can be revised to a more compact and more rigid layout, solving the current limitations of the two-circle goniometer design. However, this would be a significant design effort and a rebuild of the diffraction instrument would interrupt the user operation.

Many user experiments use the scanning-WAXS setup. In the current state, the Pilatus2 1M detector is placed on a static support of aluminum profiles, which makes the placement of the detector at the beginning of a user experiment at the desired distance time consuming. A dedicated adjustable support would reduce the installation and alignment time significantly. Also, a beam stop with an integrated photo diode will give reliable information about the transmission of the sample. The Pilatus2 1M detector was already used at MAX-lab. A replacement would increase the count rate and improve the reliability. Currently, no funds have been secured for a detector replacement.

For various experiment the XRF signal of the sample is of crucial interest. The originally installed, Ge-based XRF detector had to be removed from the setup, because its built-in cryostat caused unacceptable vibrations. Currently, a SDD detector is used as XRF detector and is installed on a temporary mount. Since the place of the Ge detector in the through hole of the goniometer became available, the SSD detector can be mounted permanently in this position.

The two available optical microscopes are currently used for sample navigation and also for the optical pre-alignment of the center of rotation of the goniometer. The alignment of the φ rotation axis with respect to the KB focus can be simplified with a third optical microscope looking along the φ rotation axis. To maintain easy access to the sample area, the third optical microscope needs to be removable, e.g. via a kinematic mount.

The current Merlin read-out electronics is limited to a maximum burst acquisition rate of 1200 Hz for 1 s. The complete transfer of the burst data to the storage system takes approximately 5 s to 6 s. This is a significant limitation of the duty cycle and limits the processes that can be observed with the current system. The newly developed read-out electronics for the Merlin

detector can read 1620 frames per second continuously. When only one quadrant is read, the sustainable frame rate increases 6400 Hz. NanoMAX has applied for the funding of the new read-out electronics. Pending the approval, the read-out electronics is expected to be available for user operation in early 2022.

4.3 Workflows and online analysis

To allow users to leave the beamline with at the very least pre-processed data and where possible even reconstructed data sets, the online analysis of data is required. So far we provided (python) scripts for the reconstruction of data once a scan is finished. This included the fitting of XRF spectra, the integration of regions of interest on a 2D detector, the map generation from scanning microscopy data and ptychographic reconstructions. These scripts are designed to also be usable for the users once they left the facility to re-run these steps with tweaked parameters long after the beamtime ended.

The recent introduction of the streaming solutions for the detectors, together with the streamed output of the control software *Contrast* form the basis for real online data analysis [14]. The availability of the detector information and the meta data about the scan everywhere in the MAX IV network as they come in allows for the development of modular tools that can be used both for the existing versatile diffraction and future more stringent tomography endstation.

The first tool we have developed on the base of those streaming options was a live XRF viewer [14], which listens to the control software *Contrast* to know when scans start/stop and at which positions the exposures are performed, and also to the stream of the XRF detector to grab the raw spectra. Using regions of interested defined in a config file, the raw spectra are integrated over these ROIs. 2D maps are created for each of the ROIs, which are then shown to the user and also saved to disk once a scan finishes. The streaming solution allows to run multiple instances of this script on multiple computers in the network with different settings without hindering each other.

It is planned to expand this tool by separating the calculation of the scalar values for each scan position, the 2D map creation and the viewer for the users into three tools which in turn also stream (and save) their results. This way this system can be easily expanded to show 2D maps of fitted XRF spectra, radially integrated XRD data or any other streamed and further processed value by simply adding another script that calculates the scalar data for those contrasts. The separability is also chosen to allow for scaling the compute requirements as needed. In recent tests we have confirmed that our solutions for compute heavy tasks such as radial integration of 2D data, creating cake diagrams of XRD data, binning of 2D data are able to keep up with the incoming data streams even at the highest frame rates of all detectors currently present at the beamline [14]. The functionality of being able to re-run the whole analysis post beamtime will be kept.

More advanced reconstructions of for example ptychographic data sets also profit from these streaming solutions. *Contrast* is designed to allow for the addition of arbitrary keyword arguments in its scan commands. Currently this functionality is used to add Boolean markers to trigger the execution of another script, for example the automatic creation of a job with *SLURM* on the compute cluster to run a reconstruction of that specific scan, once the scan has finished and this keyword argument has been part of the scan command. The Boolean variable can easily be exchanged to be a file path to a config file which shall be used for a reconstruction. There are also developments towards real-time reconstructions, where the user does not have to wait for the scan to finish to see an intermediate result, as described in Section 3.4.5.

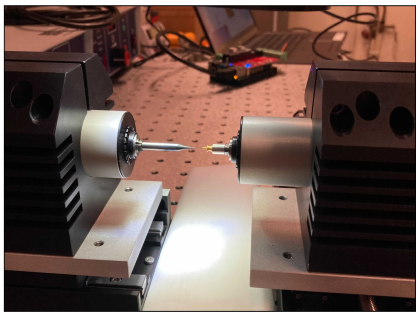
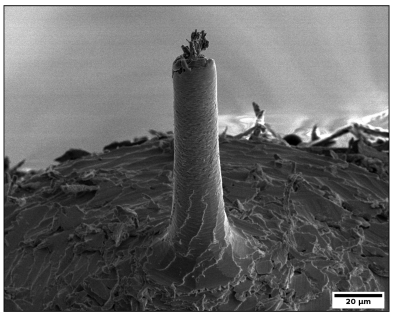

Figure 23: Left: photo of the current development status of the NanoLathe sample preparation setup with the milling tool mounted on the left and the OMNY pin with the sample to be milled mounted on the right. Right: SEM image of a prepared test sample cylinder with 18 µm diameter. (Both images by Olivia Messler)

4.4 Nano-Lathe for rapid tomography sample preparation

The upcoming tomography endstation will be more restrictive when it comes to sample sizes, shapes and mountings. It is planned to have samples mounted on OMNY pins [4]. Flat samples for 2D imaging can easily be mounted on Si_3N_4 membranes, which in turn are mounted on an OMNY pin for flat samples. Samples for tomography however need to be of a cylindrical shape and mounted at the tip of a pointy OMNY pin. So either a sample is already cylindrical and has an appropriate diameter or it needs to be shaped into a cylinder of the appropriate size. Preparing and mounting these cylinders of a few micrometer diameter is often done using a FIB microscope. This process allows to choose a specific region of the sample to be extracted, prepared and mounted, but comes at the cost of long preparation times, the need for extensive training and access to a FIB microscope in the first place.

To allow the easier and faster preparation of samples for which the choice of the very exact sub-region of a larger sample is not that critical, we adapted the idea of building a Nano-Lathe setup [24]. A master student at KTH Stockholm (in the group of Prof. Ulrich Vogt) is currently developing, testing and documenting sample preparation protocols using this device (see Fig. 23), which will afterwards be returned to the NanoMAX beamline, where it will be accessible for users to prepare large quantities of tomography samples prior to and during their beamtimes.

References

[1] U. Johansson, *In preparation* (2021).

[2] U. Johansson, et al., *Microsc. Microanal.* **24** (2018), 252.

[3] S. Zhang, et al., in *Proc. of International Conference on Accelerator and Large Experimental Control Systems (ICALEPCS'17), Barcelona, Spain, 8-13 October 2017*, number 16 in International Conference on Accelerator and Large Experimental Control Systems, JACoW, Geneva, Switzerland (2018), pages 143–150, https://doi.org/10.18429/JACoW-ICALEPCS2017-TUAPL05.

[4] M. Holler, et al., *Review of Scientific Instruments* **88** (2017), 113701.

[5] A. Björling, et al., *J. Synchrotron Radiat.* **26** (2019), 1830.

[6] L. A. B. Marcal, et al., *ACS Nano* **14** (2020), 15973, pMID: 33074668.

[7] M. Osterhoff, et al., *J. Synchrotron Radiat.* **26** (2019), 1173.

[8] A. Björling, et al., *Opt. Express* **28** (2020), 5069.

[9] L. Chayanun, et al., *Nano Lett.* (2020).

[10] P. Thibault, et al., *Ultramicroscopy* **109** (2009), 338.

[11] P. Thibault, et al., *Nature* **494** (2013), 68.

[12] P. F. Tavares, et al., *Journal of Synchrotron Radiation* **25** (2018), 1291.

[13] E. Griesmayer, et al., *AIP Conference Proceedings* **2054** (2019), 060052.

[14] A. Björling, *Submitted* (2021).

[15] http://www.github.com/maxiv-science/contrast.

[16] M. Kahnt, et al., *Journal of Applied Crystallography* **53** (2020), 1444.

[17] B. Enders, et al., *Proc. R. Soc. A* **472** (2016), 1.

[18] V. Solé, et al., *Spectrochim. Acta Part B At. Spectrosc.* **62** (2007), 63.

[19] V. Favre-Nicolin, et al., *J. Appl. Crystallogr.* **53** (2020), 1404.

[20] J. Kieffer, et al., *J. Phys. Conf. Ser.* **425** (2013), 202012.

[21] A. Björling, et al., *Phys. Rev. Lett.* **125** (2020), 246101.

[22] S. Sala, et al., *submitted* (2021).

[23] R. Akan, et al., *Micromachines* **11** (2020), 301.

[24] M. Holler, et al., *Journal of Synchrotron Radiation* **27** (2020), 472.

A Full user feedback

Report submitted	Support comments
26/03/2018	During the night there is no support at the beamline, so major issues cannot be resolved.
27/03/2018	Fantastic support throughout and after the experiment!
10/04/2018	Fantastic staff!!!
20/04/2018	I found the support excellent, see comment after point 6..
21/05/2018	Generally all staff was very helpfull and did everything to try to solve the problems we had.
22/05/2018	Very helpful and kind staff, clear and well structured!
05/07/2018	Excellent support by the staff scientist responsible for the experiment. Great support from the technical support to have the diamond phase plate installed (including motorization and design of the diamond manipulator). I have found clumsy the procedure to get a gas bottle of Helium as we had to wait almost a day to receive it.
11/12/2018	The support was great!
07/01/2019	We got excellent scientific and technical support during the experiment
07/01/2019	Excellent support by the beam line scientist.
21/02/2019	Excellent support
04/04/2019	The support was excellent and very competent.
22/05/2019	Very friendly and helpful staff.
05/06/2019	Beamline scientist was with us even during weekend. We got trouble-shot supports over the phone even it was 11:30 pm in late night. We have no more to say than greatly appreciate all the supports which we have received from the beamline scientist (Alexander Bjorling) and the engineer (Sebastian Kalbfleisch). Meanwhile, we got thorough discussions with both Karina Thånell and Alexander Bjorling regarding the feasibility and the setups of the beamline before arrival for preparing the experiments and fabricating the customized parts. We greatly appreciate these discussions too.
02/07/2019	The local contact did a wrong installation or setup of the piezo motors we were going to use, we spent 3 hours trying to debug the problem and after when we found the problem we spend 8 hours of the night waiting for the local contact to come to set the piezo properly at 9 am, that took 2 hours so at 11 we could continue with the experiment. So a total of 13 hours lost because the setup was not done carefully at the beginning. Alexander, who was not involved in the local contact duties, helped a lot in running the online ptychographic reconstruction, we thank him for this effort, even he was tired from his beamtime the week before ours, I think this shows that Alex is really devoted to the beamline and the user support working in the late evening from home to deliver a upgrade code for our needs.

Continued on next page

Report submitted	Support comments
02/09/2019	Our local contact Ulf Johansson was perfect for the organization of the beamtime, despite the experiment being very demanding in terms of equipment. Even if I was bringing equipment from my own everything was working smoothly at the beamline thanks to perfect organization. The local contact didn't get very involved in the project scientifically, but this was probably a choice, as there was sufficient staff that had worked previously in NanoMAX involved in the experiment. So a scientific involvement was not expected and anyway not needed.
08/11/2019	Problems with permissions to our run directory that could not be fixed by technical staff, needed to run from staff directory Also, see problems with data transfer from detector above
18/11/2019	Very competent staff.
12/12/2019	Excellent support
13/12/2019	We had great help with sample preparation and good support during the experiments.
18/12/2019	Excellent support!
02/01/2020	Excellent support for a relatively complex experiment.
09/01/2020	Overall a great local contact.
14/04/2020	To minimize the risk of catching coronavirus during traveling (e.g., by train), Alexander Björling (the contact beamline scientist) agreed to run the experiments for me. He did an excellent job during the data collection. After the experiment, he also provided strong support in term of data transfer, visualization and treatment. I really appreciated his strong support and commitment!
28/07/2020	Super support!!
05/08/2020	Excellent support from Ulf Johansson!
04/09/2020	Local contact was kind, helpful, and in general very available.
25/09/2020	Fantastic support!
18/10/2020	Could not be any better, absolutely great!

Report submitted	Beamline comments
26/03/2018	During our experiment, the SPOCK session was interrupted several times. We had to restart devices in TANGO, and sometimes it did not help. It was unclear how to get the control back without staff help.
27/03/2018	Overall the experiment went well and everything around the beam was much more stable compared to last year. There is still a bit more work to be done regarding instructions /documentation to help users run by themselves as well as to write scripts to convert data for futher processing etc. However, since that was not in place, we had excellent support from the beamline staff instead, and afterwards, we've had help converting data as well.
10/04/2018	Scripts for standard data reduction (diffraction with area detectors) would be useful. Stable beam with excellent performance.

Continued on next page

Report submitted	Beamline comments
20/04/2018	The N/A rating for item 7. is due to the fact that I could not do some data analysis on-the-fly that would have served me to test the beam stability, so I cannot comment on that (yet), as the analysis is not finished. This failure is related to the issue above reg. data transfer: I could not access the data during the exp. The sample environment was OK for our experiment, we did not need any complex setup. Overall, the beamline control was also fine. Data processing, I cannot comment as I was using my own software, but the utilities for data visualisation were OK. I did not have to access the beamline documentation as all the info we needed was provided to us by the local contact
21/05/2018	Crashes of the control software resulted in loss of >1 day of beamtime, this software stability issue was a very severe problem. Beamline endstation, data processing and documentation was generally good, but given the young age of the beamline it can still be improved in terms of stability (first) and capabilities (second pri).
21/05/2018	See experimental report
05/07/2018	We experienced severe problems with the beamline control software of the beamline. Data acquisition software was continuously crashing making very challenging to acquire complete data sets. Hardware for image reconstructions should be improved. Intensity of the incoming X-rays was changing up to 20% over time, an intensity monitor before the sample has to be installed.
11/12/2018	It was working well, but I wouldn't have been able to perform any measurements without a member of staff from the beamline.
07/01/2019	I would like to be provided with access to data via Duo (I have no access to data) also I would like to be provided with the access to the cluster since big data set to be able to analyze XRF data. I would suggest to provide users with a connection to the WPPM which could be granted via DUO credentials. I would need software to analyze the XRF data (now I have to ask beamline scientist for that),
07/01/2019	In addition to the beam line instrumentation per se, very help with the optical microscopes for grid/sample analyses.
18/02/2019	Detector arm must be improved: reproducibility, computer control, implement HKL mode...
21/02/2019	Better reliability of the robot detector arm would be great
11/03/2019	It is great to come back after a year and see the developments that have taken place. Lots of big and small improvements every time. The documentation for users e.g. manuals etc, still needs a bit of work to make it more userfriendly and make users more independent, but the continuous support by the beamline staff ensure that you do not yet miss those instructions.
27/03/2019	We had some issues with disappearing data that was quite unnerving

Continued on next page

Report submitted	Beamline comments
04/04/2019	Overall, the experiment was succesful. The focus was very stable in itself. The energy scans worked very well. Nanomax is very well designed for such experiments, with the secondary source and the feedback system. The detector robot worked very well. It's a pretty unique ability to be able to scan a detector so quickly. Some calibration work is needed, both to improve and to measure the precision of the robot. The thermal stability and the drift were much better than our experiment a year ago. Still, it was obvious that the thermal drift is still the dominant source of mechanical instability, so I would recommend that even more effort is put into this aspect. The Sardana system was not so stable, and it was by far the largest source of instability with about 5 crashes per day on average. We had to restart scans a few times. This makes it impossible to make long acquisitions spanning more than a few hours.
07/04/2019	The beam/sample stage stability is low on sub 100 nm level. A lot of evident drift between scanning lines.
22/05/2019	The online logbook is not good at all. We had problems with multiple open windows and it is difficult to copy images / screen shots into the logbook. A paper version would be nice.
05/06/2019	The beamline setups are perfect for us. Very clean and small X-ray probe was delivered, which is crucial for our experiments. The online optical systems and motor systems allow easy locating our sample in special diamond anvil cell environment and the collection of single crystal diffraction data with high position reproducibility. Beamline softwares allow easy performing XRD contrast mapping and the analysis software performs immediate data reduction to plot the map we just finished measuring. It is amazing. The control software is easy to learn once one gets some hand-on experiences.
04/07/2019	The control software is not very stable
02/09/2019	The Sardana software was crashing all the time, up to 10 times a day. I was lucky because I came to do experiments with experienced collaborators who had worked at NanoMAX before, but without them I would have been lost. And I consider myself an experienced synchrotron user. I was impressed by the online processing tools for data visualization and ptychography. Documentation seems to be also very good by what I could see, although I didn't have to use it myself.
04/11/2019	Problems with the stage for meant that the collected maps were not really usable due to too large and erratic "drift".
08/11/2019	Beamline alignment and performance worked well
18/11/2019	Pilatus 1M detector server kept needing restarts, which was annoying. Very much looking forward to the Eiger 4M detector being in place.
09/12/2019	We were very impressed with the NanoMax beamline. Obviously it is a fairly new beamline that is still in its infancy, but considering how long the beamline has been running it was very good. We managed to measure twice as much as we expected.
13/12/2019	There were some problems with the software during the mapping.

Continued on next page

Report submitted	Beamline comments
18/12/2019	The new control software is much more stable than the previous one. We had some issues with the Pilatus detector and the robot froze once. The scanviewer is great, and it would be even better if it could make a scanning XRD analysis. A couple of suggestions: - Create some way for the users to track the progress of a long script. Perhaps a function to send emails when a scan is finished? - Improve the optical microscope software. Could one have scale bars and arrows showing motor directions? A function to have electronic markers for important positions (eg COR)? This would make alignment even easier. - The useful range for the robot should be more well defined.
02/01/2020	The facility worked very well. We had stable beam.
09/01/2020	Great experience. Good software tools. And capable cluster infrastructure for on the fly insights. I also like the digital lab book. Beam resolution on the NanoMax beamline is great. However, the stability was not overwhelming. On scanning I found large shifts every now and then.
11/03/2020	The controller software had a few crashes during our beamtime and was a bit uncomfortable (which is maybe not unusual for synchrotrons). The software for data visualization "ScanViewer" had a some serious bugs, showing wrong x/y coordinates, using wrong energy intervals leading to false elements turning up in the maps. Especially the last mentioned bug seemed that it could have been fixed quickly, but we got no information that this is done by now. As agreed by the beamline operator, ScanViewer is presently not usable for data analysis. There should be a data conversion tool to be able to analyse the data with PyMCA, but this tool is not functional either. It is really a pitty, that since three weeks, we have no solution to analyse our data.
23/03/2020	Setup stability could be further improved and background scattering needs to be reduced for investigation of low-contrast samples. For the latter, the in-vacuum Eiger will considerably help.
28/04/2020	Unable to view the STXM data collected with Eiger detector with the beamline data analysis software. A software upgrade is needed to read out small ROI from Eiger frames. For a full analysis of the XRF data, we need to open the spectra in PyMCA, it is however not trivial to do so due to the data structure of the h5 files. This we will hopefully solve soon.
28/04/2020	The online logbook is not good a. Multiple open windows causes problems. It is difficult to copy images / screen shots into the logbook. A paper version would be nice.
04/06/2020	I was not involved in this bit, just sample prep.

Continued on next page

Report submitted	Beamline comments
04/09/2020	Beam stability was excellent. Setup was flexible enough so to integrate an ESRF-made heating stage, which could be controlled remotely from outside the hutch. Overall sample stability when at a Bragg angle was sufficient for reliable large-area coarse scanning diffraction maps. Custom made beamline software for visualising such maps was very good. Only downside: no direct access to the data from outside MaxIV, and no possibility of using google docs on the control computer as a logbook to be later inspected (users are forced to use MaxIV logbook software, not accessible from the outside).
18/10/2020	The server was down several times, which made it impossible to do experiments or analyze data during those times, even though the equipment was right there. If everything is operated through the server, it should be stable., otherwise there is a risk of losing valuable beam time.
27/01/2021	Online data analysis for XRF mapping is good for navigation and a first impression, more detailed XRF analysis could be included as well. Beamline is still not optimized for full-field imaging. The online logbook does not work well: high risk that information is lost when multiple persons edit at the same time.

Report submitted	Improvements comments
26/03/2018	The data could be successfully collected if there were no interruptions in the control system. The reproducibility/stability can be improved for sub 100 nm scale measurements.
27/03/2018	The experiment was successful! We really look forward to seeing what we can get out of the data.
06/04/2018	The experience in MAX IV was very good. The only suggestion is to have a nice restaurant in the institute :)
20/04/2018	I am pleased about how the experiment went, despite we had some important issues regarding data collection and transfer which resulted in an important loss of time. I cannot state for sure yet if the experiment was successful, as the data analysis (which should give us information about the beamline and sample setup stability + model sample dynamics) is still ongoing.
21/05/2018	Most aspects worked very well, but unfortunately a few crucial aspects did not work and prevented the experiment. See experimental report for details.
05/07/2018	Software problems have made the experiment impossible, we could hardly reproduce similar results gathered at the Swiss Light Source. I was expecting facing some problems as Max IV is a rather young facility, but the software issue we have experiences where far worse than\nI could have imagined.
07/01/2019	I would suggest regular workshops for XRF users.

Continued on next page

Report submitted	Improvements comments
12/01/2019	While I was happy with the actual experiment, the critical point is the reception / guest house, which is of tremendous importance: neither did the DUO registration work, nor did the app work to open the door for the guesthouse, nor was the door key for my room in the safe. This is particularly annoying and safety relevant, as there is no one around, and it is even not possible to enter a building after hours as it is standard at other synchrotrons, where the entrance hall is accessible, and/or staff around 24/24 can help. Max IV is not an environment where one wants to be locked out in winter nights.
18/02/2019	A very good beam! Some improvements about the instruments must still be done in the future. \nPlease help the staff to manage these tasks.
18/02/2019	It was really good experience with great helps from the beam scientists, especially from Sebastian at NanoMax.
25/03/2019	I was unable to join the team for the beamtime and cannot comment on the specific session.
16/04/2019	I was doubly asked the questionnaire.
05/06/2019	The experiments are highly successful. We look forward to more opportunities to visit NanoMax in the future.
19/06/2019	A comment regarding forskarshotellet: thick curtains would be nice since most of us are trying to get some sleep at odd times and the sun from the window is a hindrance to sleep.
02/07/2019	Overall the beamtime we good, we got good data. The good knowledge of the beamline by Gerardina and the support from Alex were key points for the success of the experiment.
31/10/2019	It would be good if there was a canteen for lunch and dinner.
13/12/2019	The experiment at NanoMax was very successful. We obtained a lot of data. The problem we have now is that we don't know how to process the data.
18/12/2019	We had continuous beam for the entire experiment. The focus was very stable. The new scanning stage is much more stable than the old one. We had a very productive beamtime.
09/01/2020	We have been able to gather a great deal of data in a vary brief period of time. \nBoth before and at beam time.
11/03/2020	We assume that our results are promising and give a good mark under the assumption that the analysis software problems will be solved soon.
28/04/2020	Overall a very good experience. \nSome improvement on data analysis software for immediate evaluation of collected data would be helpful. Both for STXM and XRF data analysis.
17/05/2020	Amazing friendly staff from reception to scientist!! Wonderful facilities. Thank you!
04/09/2020	We will surely attempt to come back.
27/01/2021	Improving the nanomax capacity for holography and tomography would allow for world-class full-field nano-CT.